How will the JWST short wavelength performance affect faint galaxy parameters?

Part II — 2005: Do we "Caber Toss" JWST's 1μm performance?

Rogier Windhorst, Seth Cohen & Rolf Jansen (ASU)

JWST SWG Mtg, June 15, 2005, ROE, Edinburgh, Scotland

Outline

- (1) Use the real (drizzled) HUDF Vi'z' images as input ("truth"). Should be close, given minor differences in N(z) and K_{morph} .

The 240 hr HUDF Vi'z' images are the most realistic simulation input one can use. They closely correspond to $\lesssim$20 hrs JWST images.

- (2) Convolve with the 2005 JWST PSF's (EE(1 μm)=0.74 & 0.60).
- (3) Add noise back in to exactly match the input HUDF noise level.
- (4) Run SExtractor for object finding and galaxy parameter estimation.
- (5) Evaluate impact on various faint galaxy parameters as function of JWST PSF-characteristics and wavelength.
- (6) Conclusions.

This talk received XIV *Benedictions from the highest powers in the ITAR department*

- (1) Use (drizzled) HUDF Vi'z'-band images as input ("truth")
- (2) Convolve with the suite of 2005 JWST PSF's:

```
/home/raw/jwst/05replan/orig/*fits

nircam_psfisim1_0_7um.fits  (EE(1 mu)=0.74)
nircam_psfisim1_1_0um.fits  (EE(1 mu)=0.74)
nircam_psfisim1_2_0um.fits  (EE(1 mu)=0.74)

/home/raw/jwst/05replan/opdrelaxpsfs/*fits

opdrelax_07um.fits          (EE(1 mu)=0.60)
opdrelax_1um.fits           (EE(1 mu)=0.60)
opdrelax_2um.fits           (EE(1 mu)=0.60)
```

Details of the JWST PSF-convolutions:

• In total, 10 PSF realizations were made for each case, and these were im-combined.

• All resulting PSF's are 4096^2 in size ($0\farcs030$/pix), in order to:

(a) accommodate full Nyquist sampling at 2.0 μm (although not Nyquist sampled at 0.7 and 1.0 μm).

(b) include as much as possible of the total flux (part of the cause of the large Δm_{Tot}-errors in the 2003 PSF study).

• All PSF's were centrally added to a 8192^2 bed of zero's. This ignores the small fraction of unmodeled PSF-flux falling outside the central 4096^2 images, which is now much smaller than in the 2003 PSF's anyway).

All convolved JWST images are compared in two fundamental ways:

(a) "Input" or *absolute* comparison to original HUDF images: best shows JWST+algorithm bias if S/N$\rightarrow\infty$, but exaggerates bias at low S/N.

(b) "Airy" or *relative* comparison to HUDF images convolved with (J1(r)/r)^2 (=flawless round JWST): best shows how biases get worse at smaller wavelengths and lower EE.

- All were generated on 4096^2 grid using IDL, and rebinned and embedded in a 8192^2 image below. This allows for the best comparison, since both the simulated true JWST PSF (the hexagonal features) and the simulated "perfect" PSF have gone through exactly the same rebinning process.

- The inner 8192^2 pixels of the HUDF images are used in each filter.

- After much experimenting, only the following convolution scheme worked:

(a) FFT all 8192^2 images and PSF's (since they are just too large for blunt convolution even on 3 GHz workstations).

(b) Calculate JWST HUDF simul = FFT[FFT(HST image).FFT(PSF)]

All JWST PSF's are carefully resampled onto the right pixel scale:

- PSF-profiles measured with STSDAS 'ellipse' resemble Airy patterns.
- To find the first Airy minimum with sub-pixel accuracy, a cubic spline was fit to the area surrounding it.
- The minima were found at 5.18, 5.24, 5.00 pixels respectively.
- Since the first Airy minimum should be at $1.22 \times \lambda/\mathrm{D}$, where D=5.85 m, we now know the true angular scale of each PSF.
- This determined the rebinning factor for each PSF before convolution, which are 5.16, 3.65, 1.74 for 0.7 μm, 1.0 μm, 2.0 μm, respectively.

This means that the 0.7 μm PSF has $\sim$1 pix/FWHM, due the 0$''$.03 ACS pixel scale. Hence, both 0.7 μm and 1.0 μm are sub-Nyquist.

To solve this would require $31{,}768^2$ images, which our 2004 class workstations aren't easily up to. This can be done, if really needed — each image would then be 4 Gb, they are currently 0.25 Gb.

• The HUDF Vi'z' filters map onto the 0.7 μm, 1.0 μm, 2.0mum PSF's as following:

FWHM (V606=0.606μm) $\simeq$ 0.7 μm

FWHM (i'=0.775μm) $\simeq$ 1.0 μm

FWHM (z'=0.92μm) $\simeq$ 2.0 μm

Since galaxy morphology in general only changes slowly with wavelength the first two λ's are close enough to not render the simulation invalid.

The third assumption had to be made, since the HST J+H-band images in the HUDF were too shallow to use, and had much poorer sampling than the drizzled HUDF ACS images.

The VLT K-band image (one of the deepest that exists at 35 hrs) is also useless in this regard.

• Hence, our simulation ignores the morphological K-correction between 0.9 and 2.0 μm. Given the N(z) at AB$\lesssim$29, K_{morph} is still modest.

Since faint galaxies at AB$\simeq$24–29 mag have $z_{med} \simeq$1.5–2, this is approximately correct for about half of the faint galaxy population, since the z'-band filter samples longwards of the Balmer break at both wavelengths. (K_{morph} is usually modest longwards of the Balmer break.)

For the high-z half of the faint galaxy population, this is not true, and so the real 2.0 μm K-band — had it been observed with HST — would have looked somewhat different from i'-band, although for the dominant late-type faint blue galaxy population K_{morph} effects are still small (Windhorst et al. 2002, ApJS, 143, 113, astro-ph/0204398; Taylor et al. 2005, ApJ, 630, 1–19, in press; astro-ph/0506122).

• In other words, this simulation ignores ERO's and other red objects that would have shown up in deep HST K-band images. These are important objects, but constitute only a very small fraction of N(z).

• In summary, the resulting simulations are as realistic as they can be.

• Dividing out the FFT(HST/ACS-PSF) did not work, and deconvolving out the HST/ACS-PSF with Lucy seriously distorted the image noise. Hence, the HST/ACS-PSF is NOT deconvolved out, but left in.

• Ignoring the HST/ACS PSF effects imprinted on HUDF images causes:

All objects to appear somewhat larger, approximately in quadrature by:
fwhm(V=0.61μ)=0$''$.06, fwhm(i'=0.78μ)=0$''$.08, fwhm(z'=0.92μ)=0$''$.09.

• Since faint galaxies have median $r_e \simeq$0$''$.2–0$''$.3, this is OK, although it does distorts the smallest galaxies, in the sense of making their r_e (V606=0.61μm), r_e (i'=0.78μm) look slightly better than r_e (z'=0.92μm).

The exercise is thus conservative in that it may make r_e (V606=0.61μm) and r_e (i'=0.78μm) look slightly better than than they are in reality compared to r_e (z'=0.92μm).

• THE READER IS CAUTIONED TO NOT FALSELY INTERPRET THIS.

• The only alternative is to study the algorithm behavior on artificial galaxy images (as in Jansen & Windhorst 2002), but this would have made the simulation rather unrealistic for the expected faint galaxy mix.

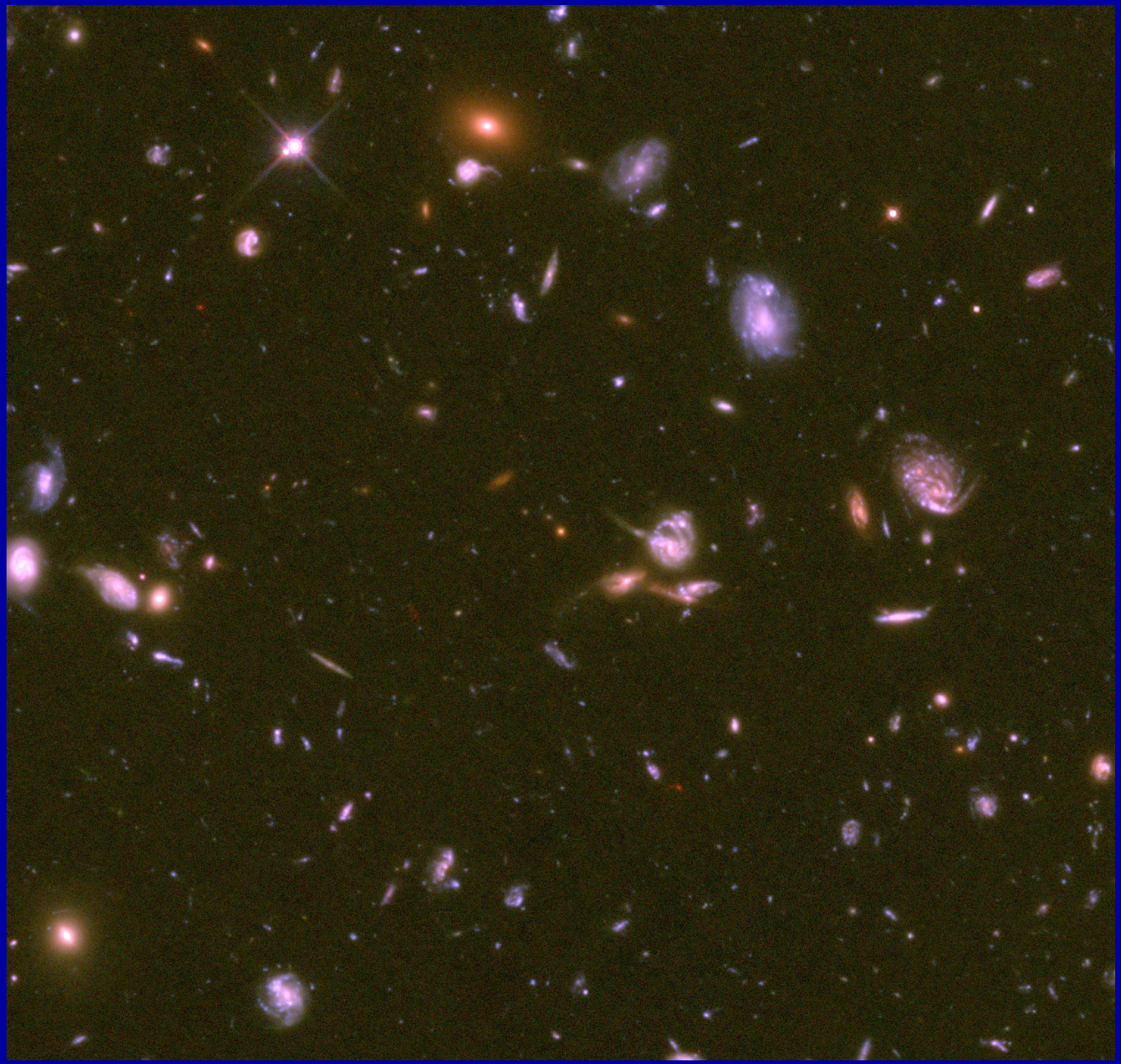

240 hrs HST/ACS in Vi'z' in the Hubble UltraDeep Field (HUDF)

6.5m JWST PSF models (Ball Aerospace and GSFC):

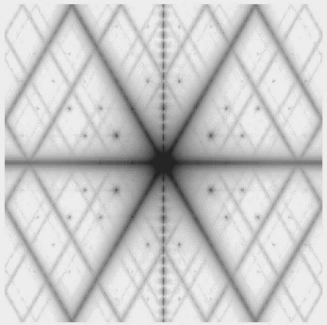

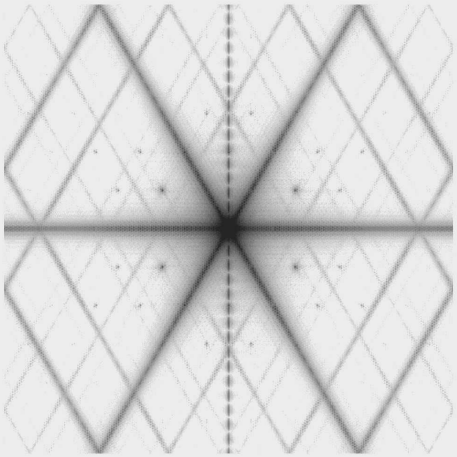

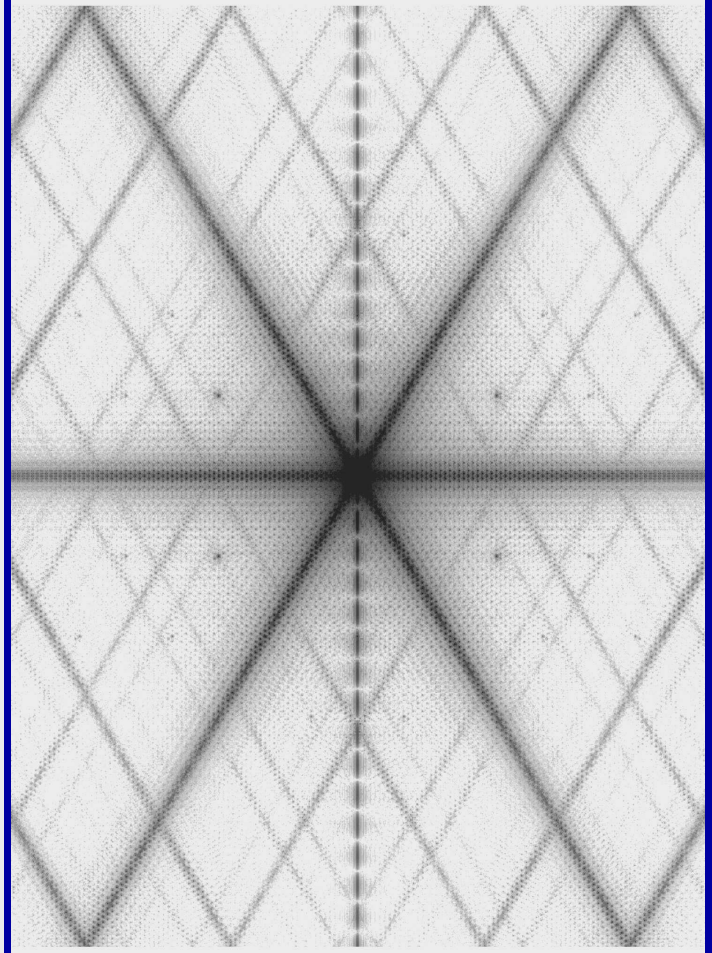

NIRCam 0.7 μm

1.0 μm ($<$150 nm WFE)
EE=0.74 (1.0μm)

2.0 μm (diffr. limit)

$\lesssim$20 hrs JWST NIRCam at 0.7, 0.9, 2.0 μm in the HUDF

$\equiv$Truth (= HUDF Vi'z') $\lesssim$20 hrs JWST 0.7, 0.9, 2.0 μm

Galaxy structure visible to AB$\lesssim$29 mag with JWST-PSF in $\lesssim$20 hrs, but contrast in the "blue" is lowered due to the short-wavelength PSF-wings.

• (4) Run SExtractor in dual image mode for faint object finding and galaxy parameter estimation.

• Unlike the 2003 simulations, LMORPHO was not run this time to get faint galaxy types, since these types are more uncertain, and this step involves a large amount of manual object editing/aperture setting.

• Corollary: we don't have true effective radii r_e or half-light radii — use SExtractor FWHM's instead. In general: FWHM $\simeq 1.8\ r_e$

• Define SExtractor apertures on the convolved images. This is only fair, since light is more spread due to the convolution (doing otherwise led to part of the significant Δm_{Tot} flux bias in the 2003 study).

• (5) Evaluate impact on various faint galaxy parameters as function of the JWST PSF-characteristics at 0.7, 1.0 and 2.0 microns. See below.

Galaxy parameters considered all came from SExtractor:

- Total magnitudes (MAG_AUTO)
- SExtractor FWHM as proxy to half-light or effective radius r_e
- Object ellipticity b/a
- Position Angle (PA) of major axis a

The FWHM, b/a, PA were NOT generated by using matched apertures, since these parameters are held constant in that case. Instead, they were obtained from separate SExtractor runs and positional cross-matching.

The PA's are only plotted for b/a$\lesssim$0.8, since they are ill determined for rounder objects, even brighter ones.

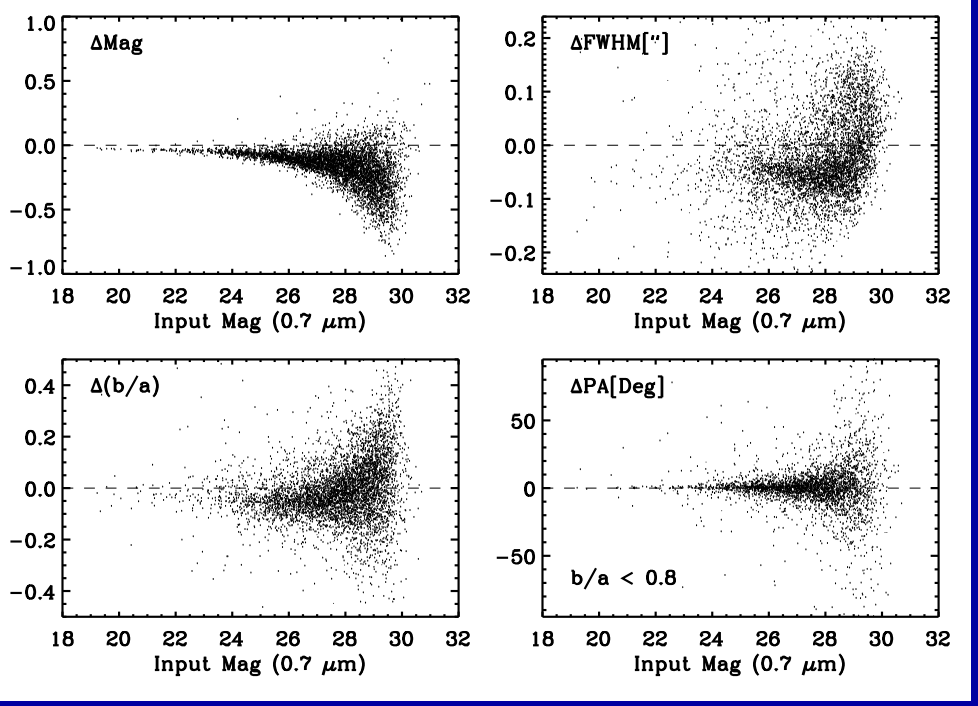

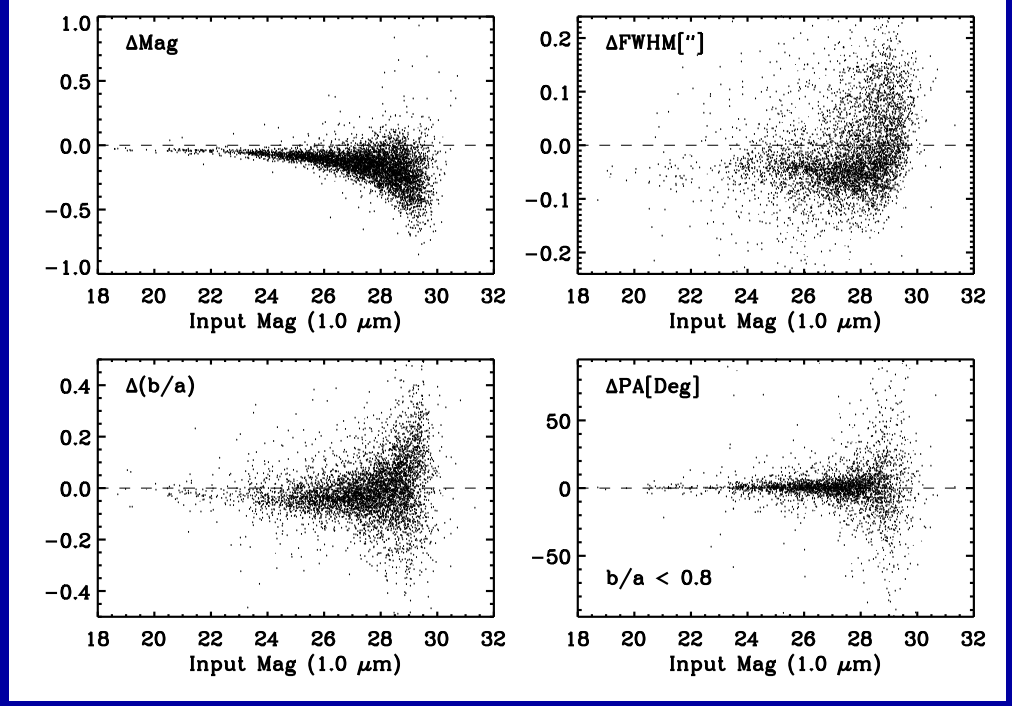

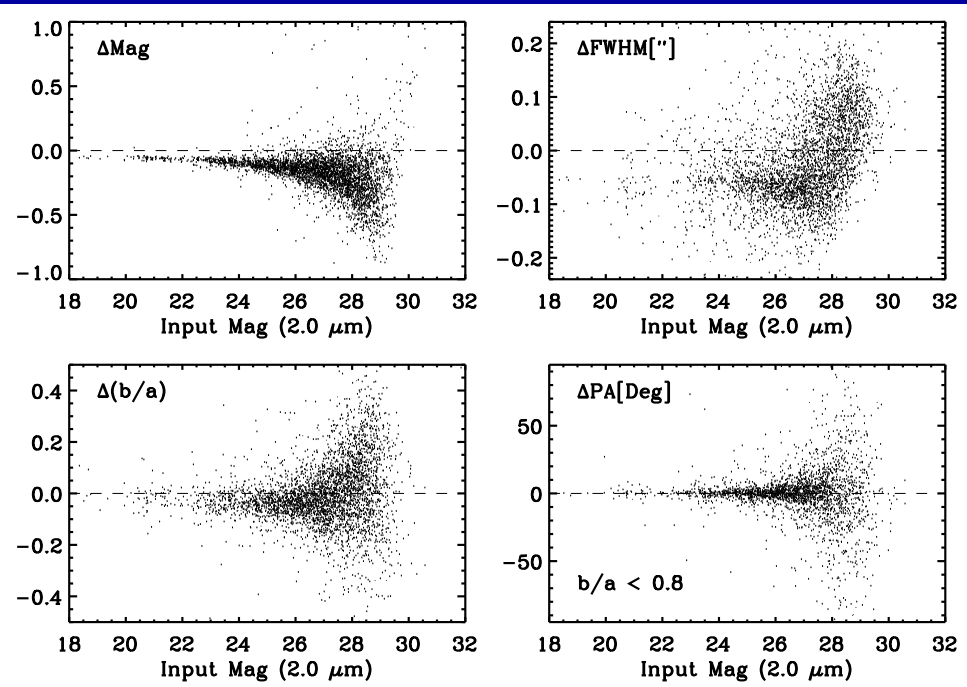

Input–JWST: EE(1.0μm)=0.74

Δm_{Tot} ΔFWHM

Δb/a ΔPA

0.7 μm 1.0 μm

2.0 μm

PA-bias is modest & largely random.

m_{Tot}, fwhm, b/a-bias significant,

and caused by algorithm's response to PSF-wings. For real JWST images, it is *this* bias that has to be modeled and removed (*not* the Airy-bias).

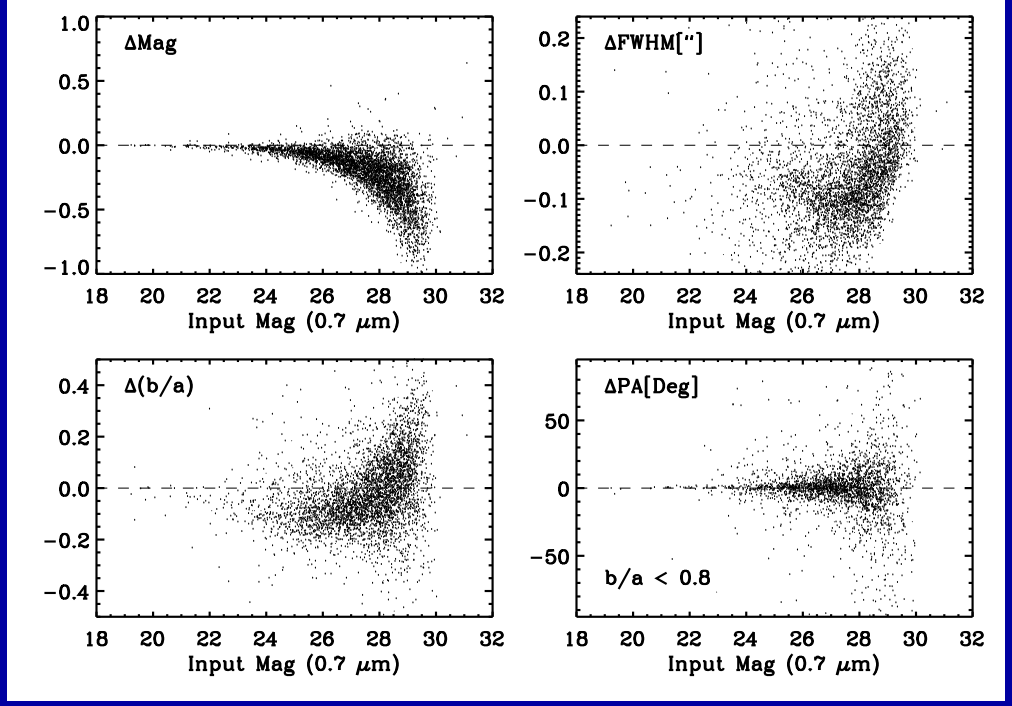

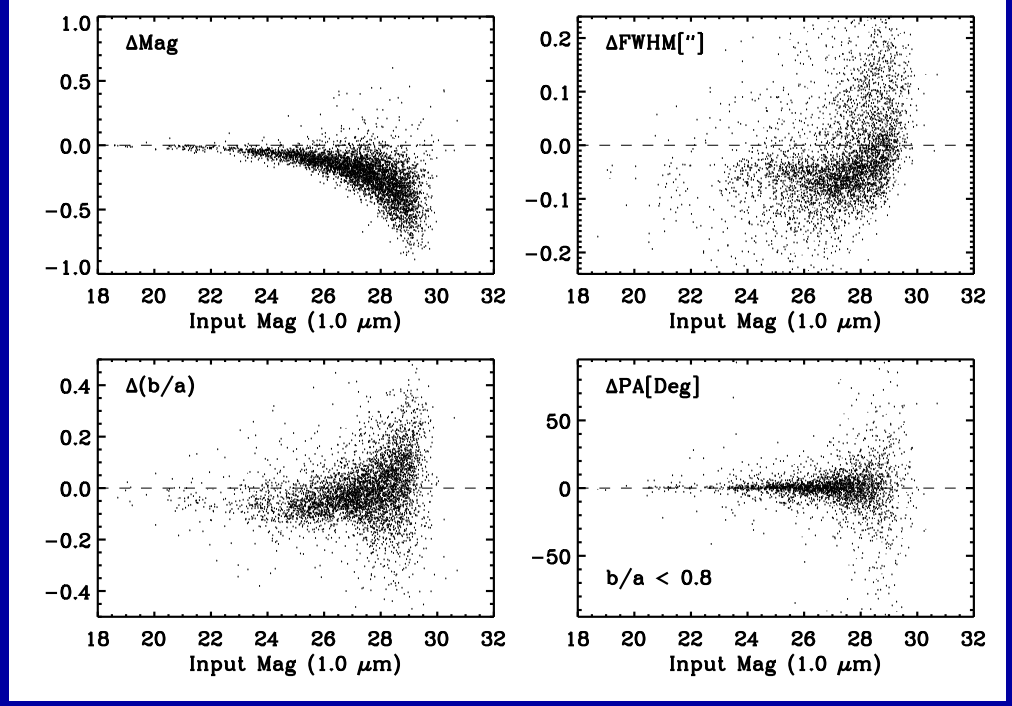

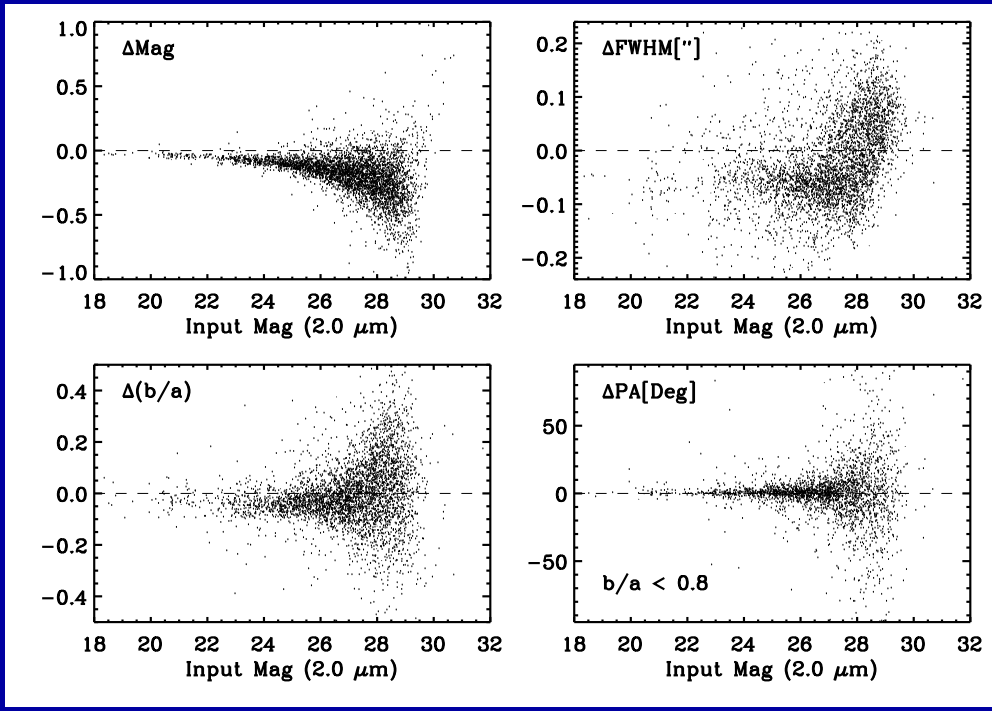

Input–JWST: EE(1.0μm)=0.60

Δm_{Tot} ΔFWHM

Δb/a ΔPA

0.7 μm 1.0 μm

2.0 μm

For EE=0.60, PA-bias modest & random. The m_{Tot}, FWHM, and b/a-bias become much more significant at 0.7 μm, 1.0 μm, but are held ∼constant at 2.0 μm (as spec-ed!).

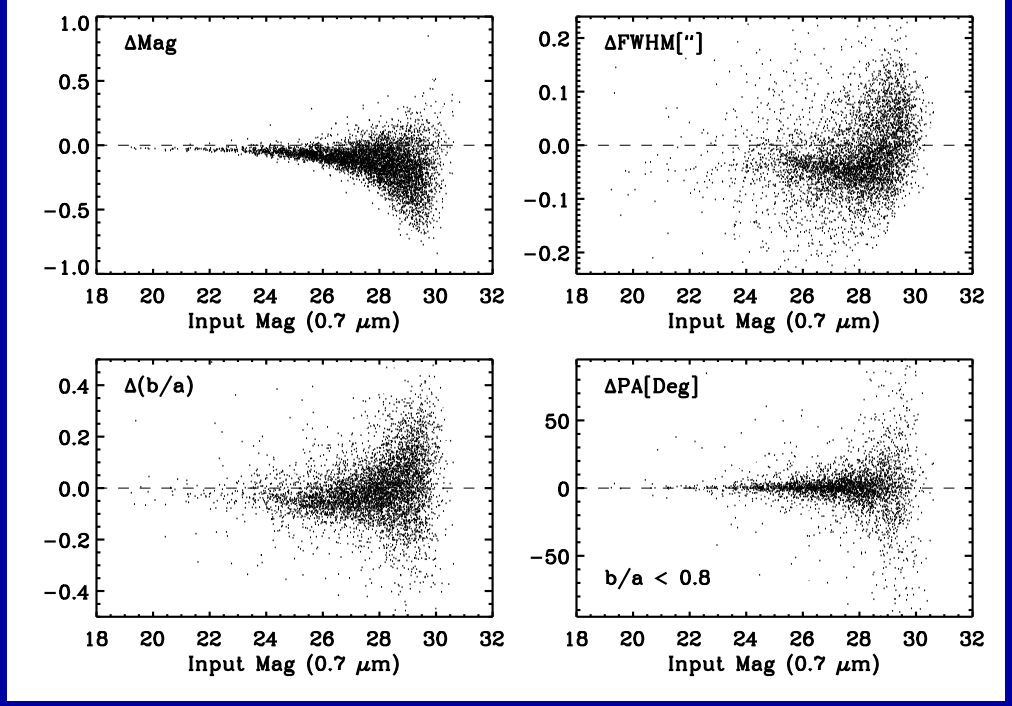

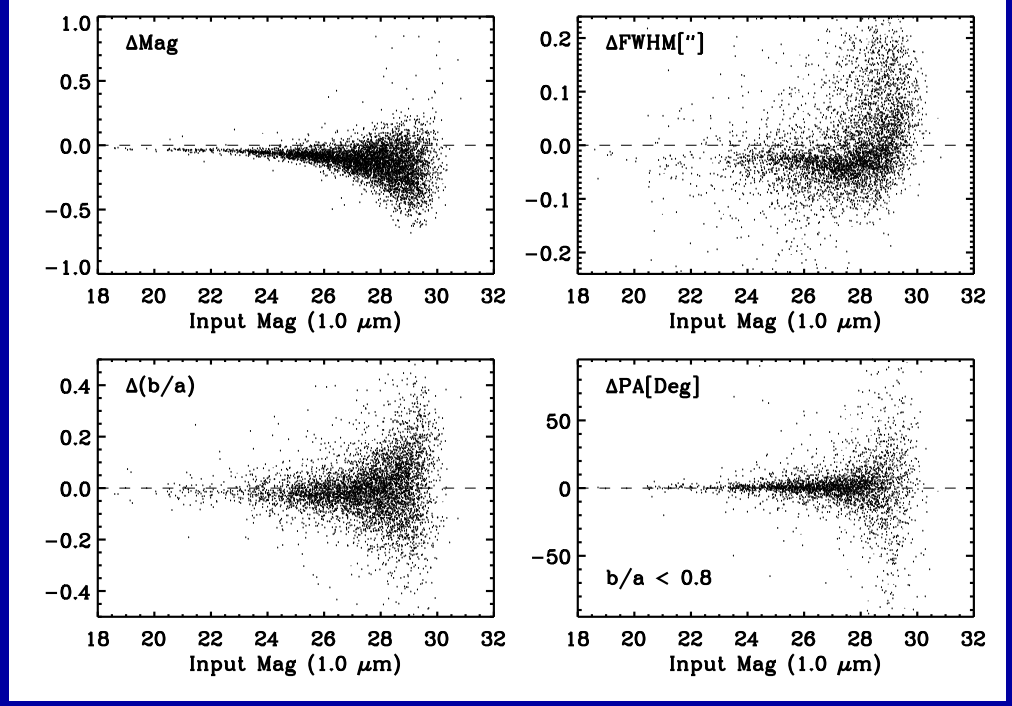

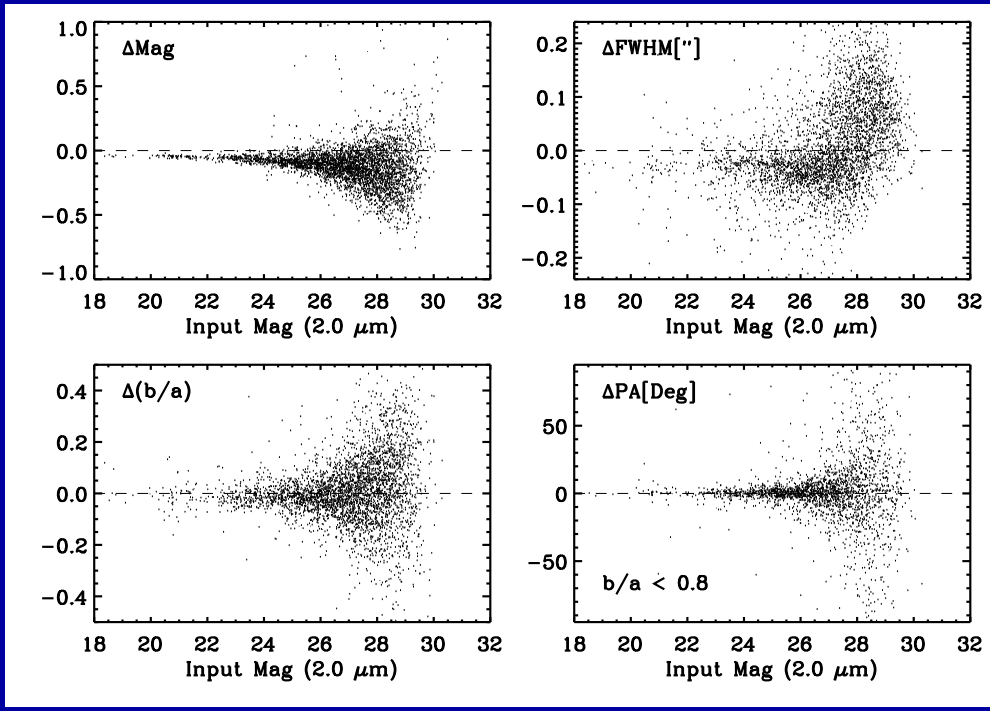

Airy–JWST: EE(1.0μm)=0.74

Δm_{Tot} ΔFWHM

Δb/a ΔPA

0.7 μm 1.0 μm

2.0 μm

Relative PA-bias modest & random.

The m_{Tot}, FWHM, b/a-bias is still significant, and caused by algorithm's response to real PSF-wings (as compared to its response to an Airy function).

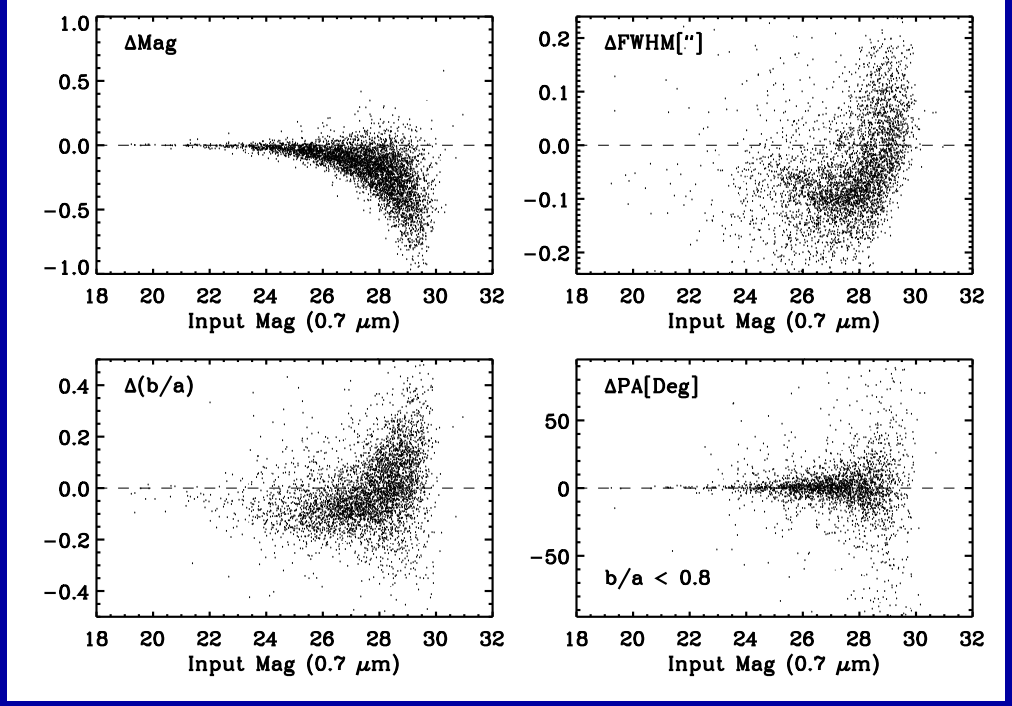

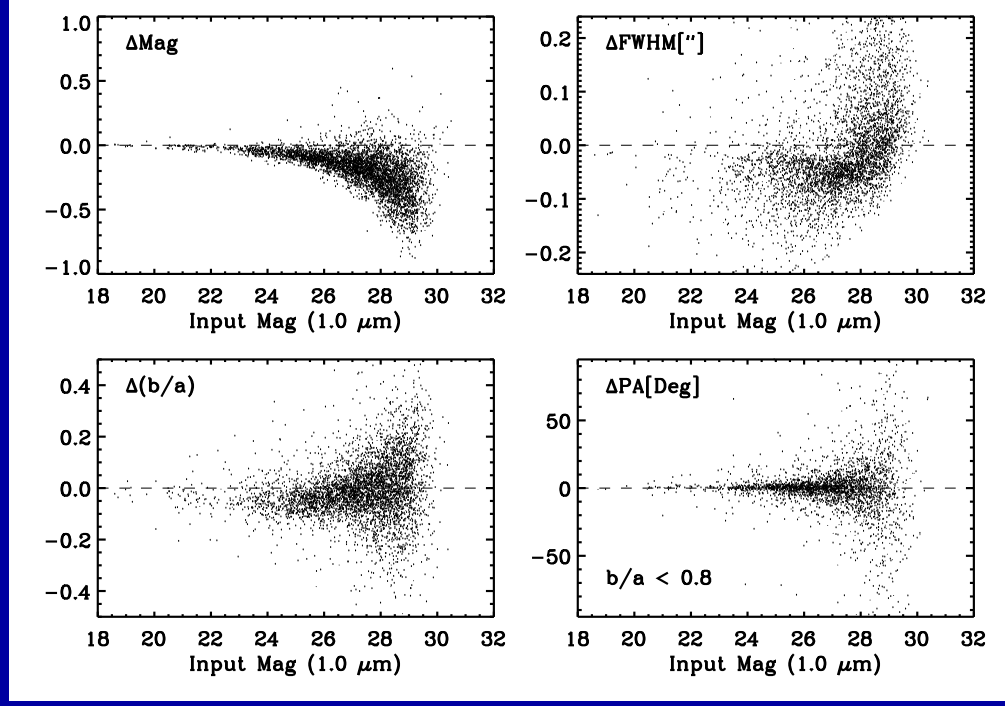

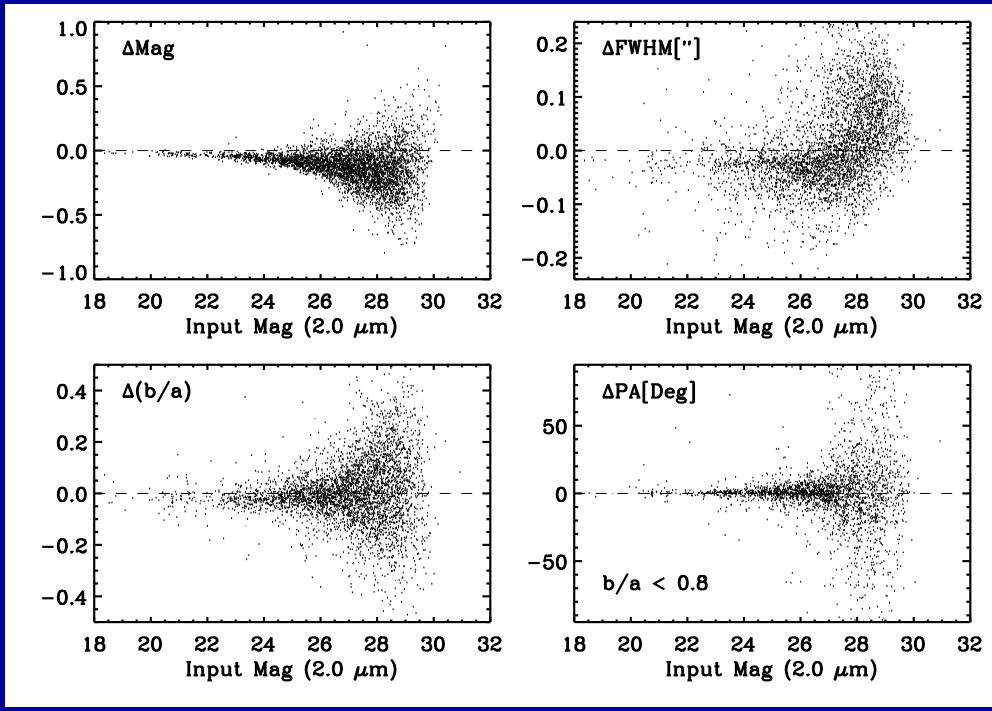

Airy–JWST: EE(1.0μm)=0.60

Δm_{Tot} ΔFWHM

Δb/a ΔPA

0.7 μm 1.0 μm

2.0 μm

For EE=0.60, the relative PA-bias remains modest & random.

The m_{Tot}, FWHM, b/a-bias become much more significant at 0.7 μm, 1.0 μm, but are held ∼constant at 2.0 μm (as spec-ed).

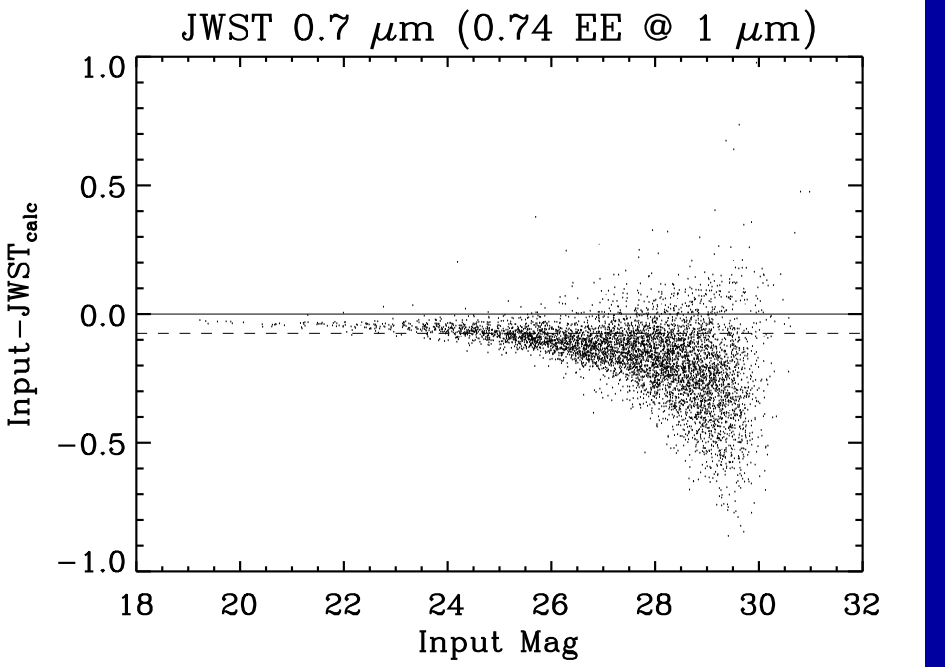

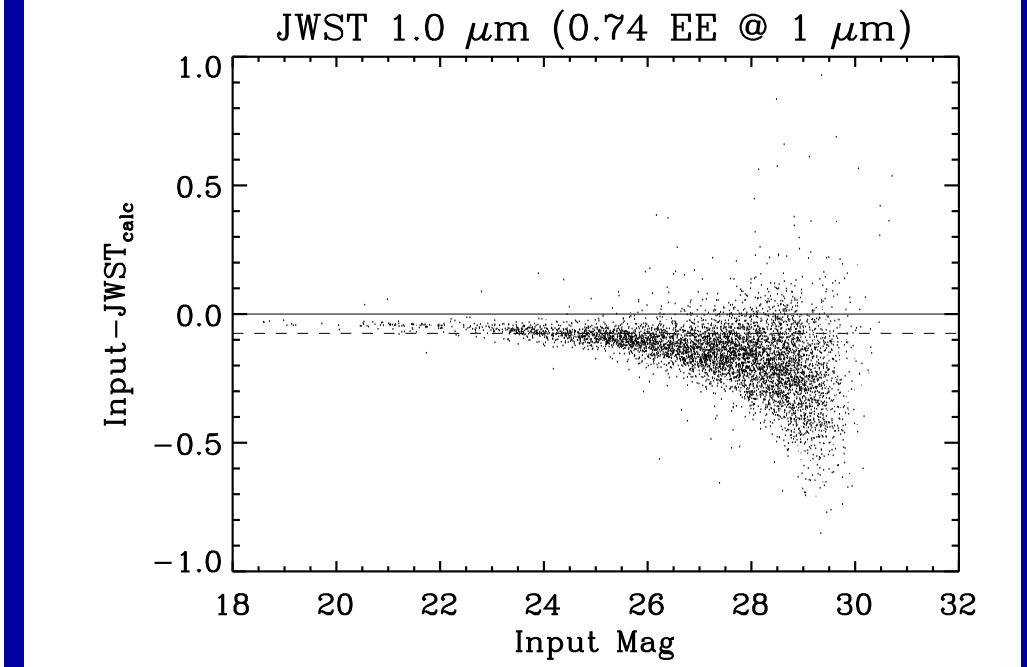

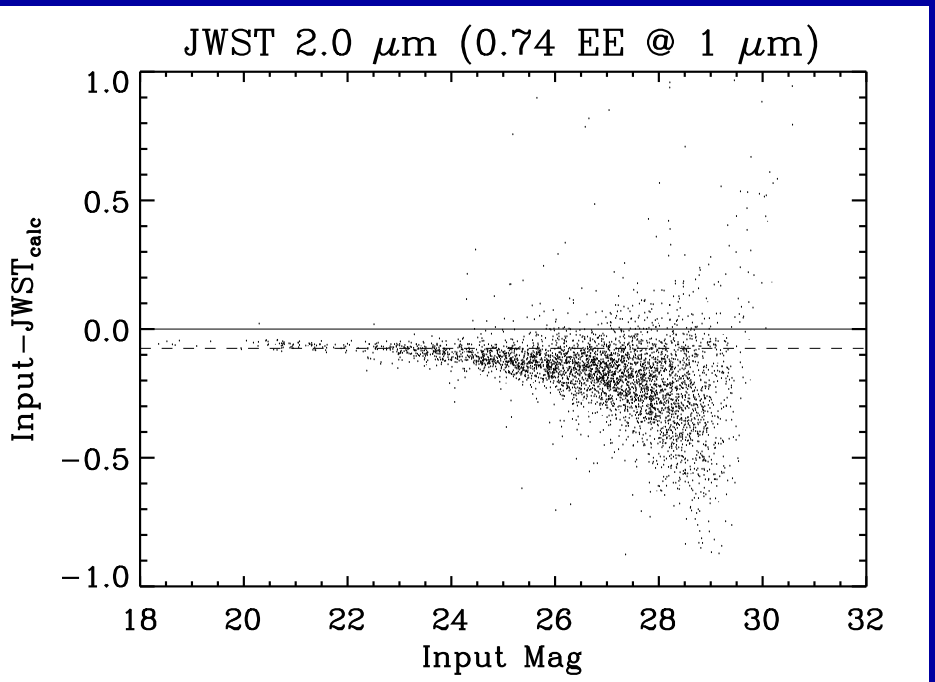

Input–JWST: EE(1.0μm)=0.74

Δm_{Tot}

0.7 μm 1.0 μm

2.0 μm

m_{Tot} bias is significant, and is still –5% at very bright fluxes, but for EE=0.74, the 1.0 μm bias is slightly better than at 2.0 μm (due to better λ/D), & at 0.7 μm not much worse (but limited by undersampling). Must model and remove this bias.

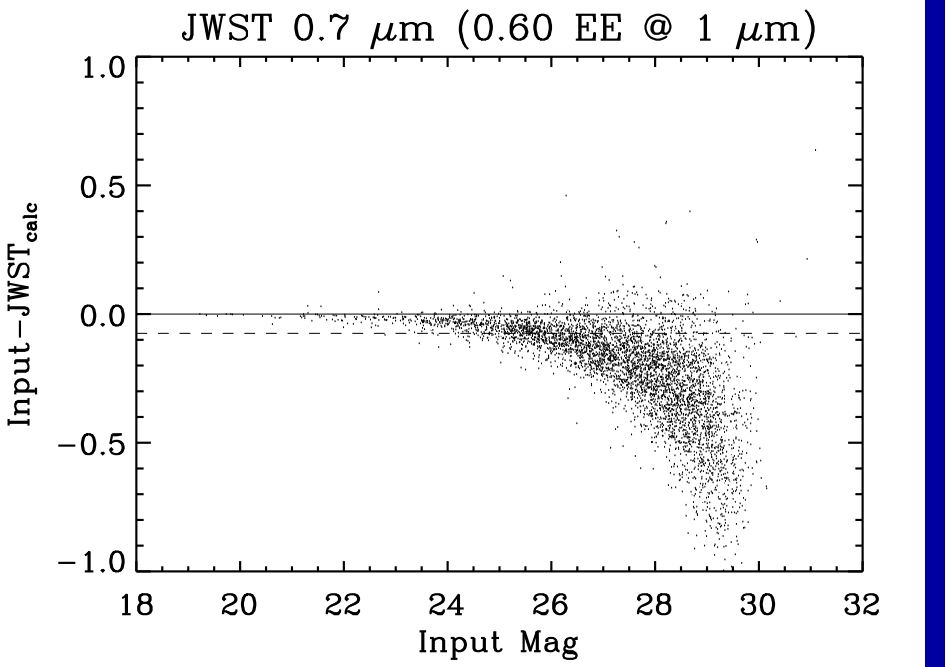

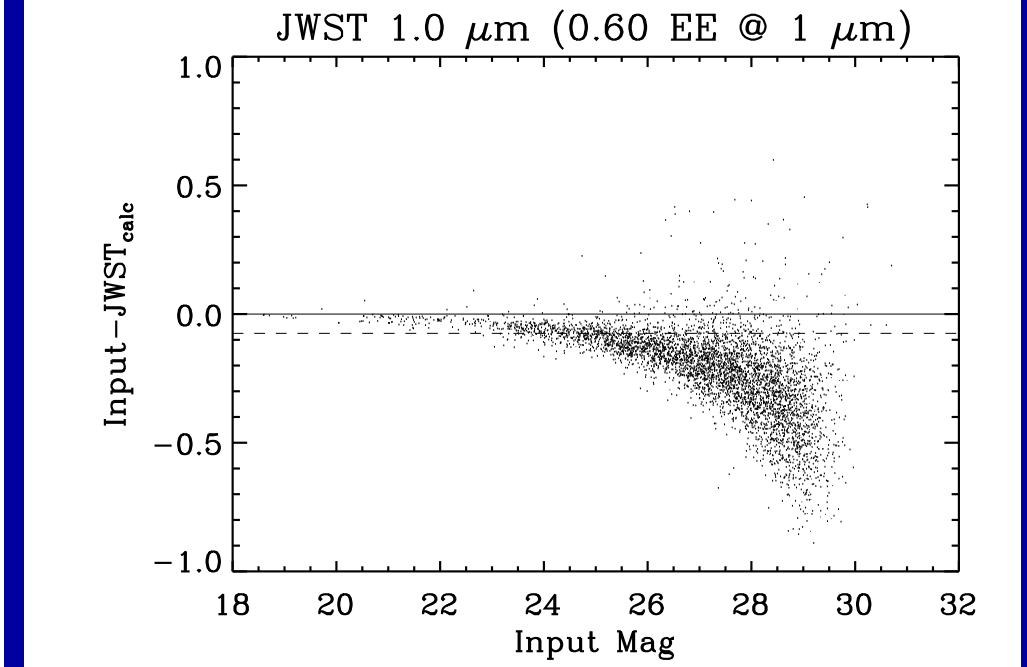

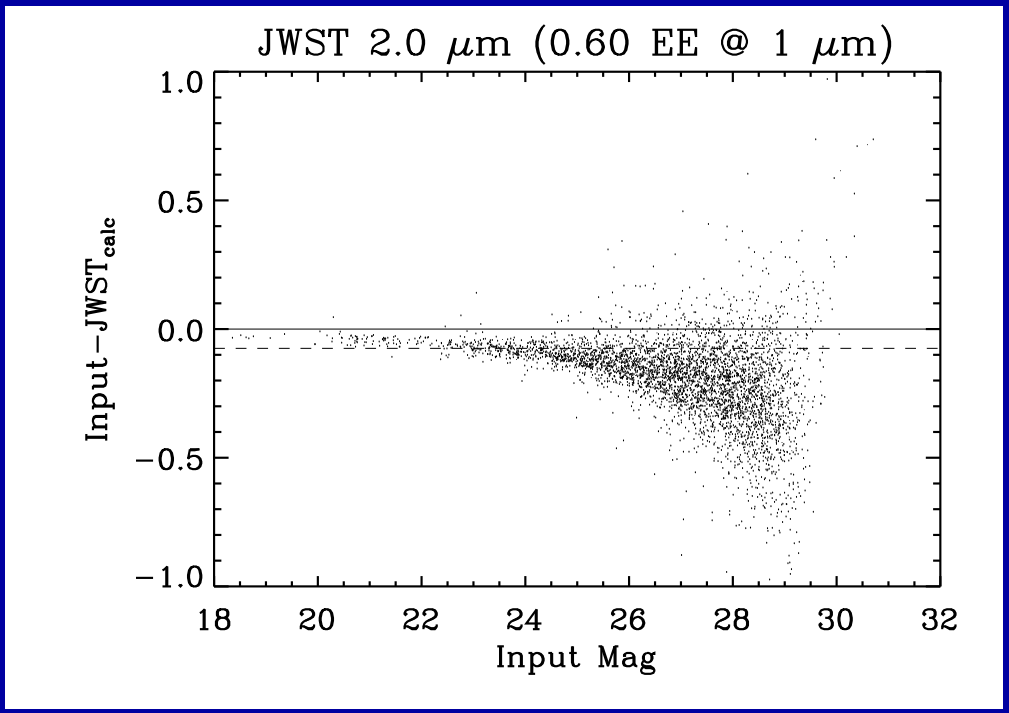

Input–JWST: EE(1.0μm)=0.60

Δm_{Tot}

0.7 μm

1.0 μm

2.0 μm

For EE=0.60, the m_{Tot} bias gets more significant, especially at 0.7 and 1.0 μm. Effects from better λ/D at 1.0 μm are no longer seen. 2.0 μm performance is held $\sim$constant. Must remove these biases from the real JWST images.

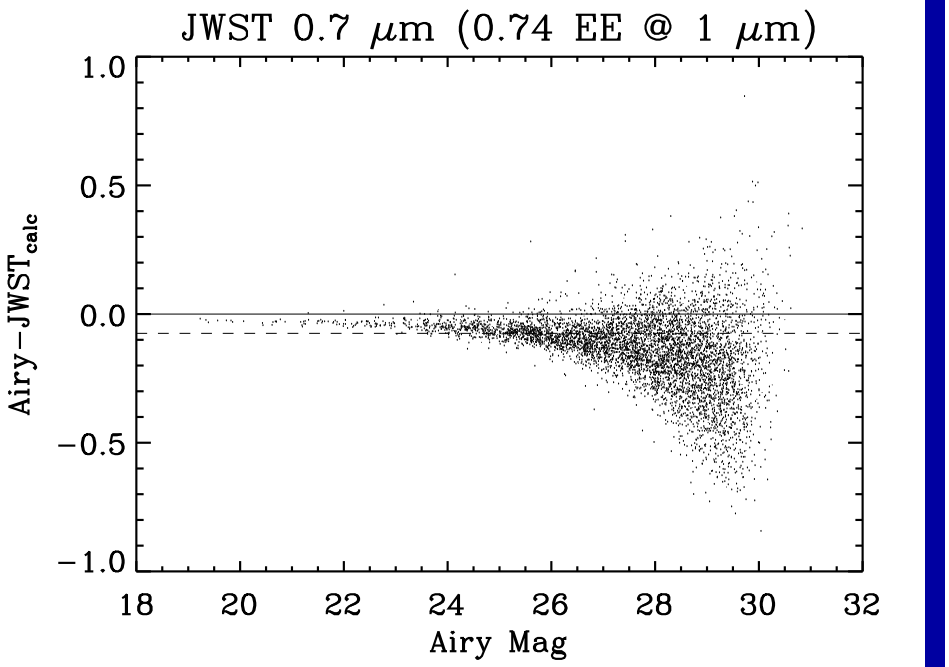

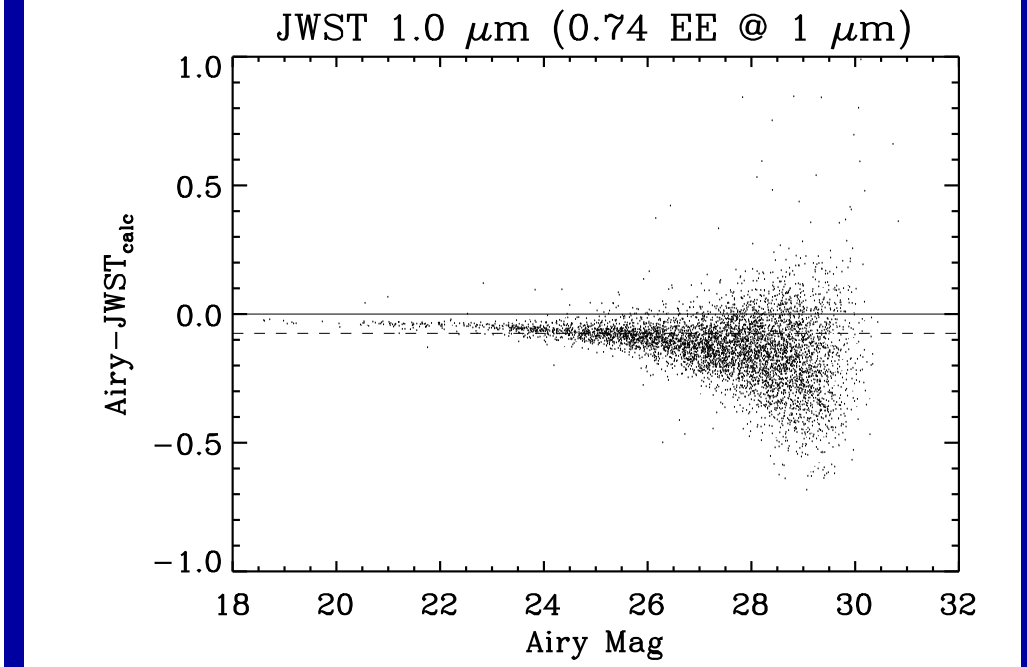

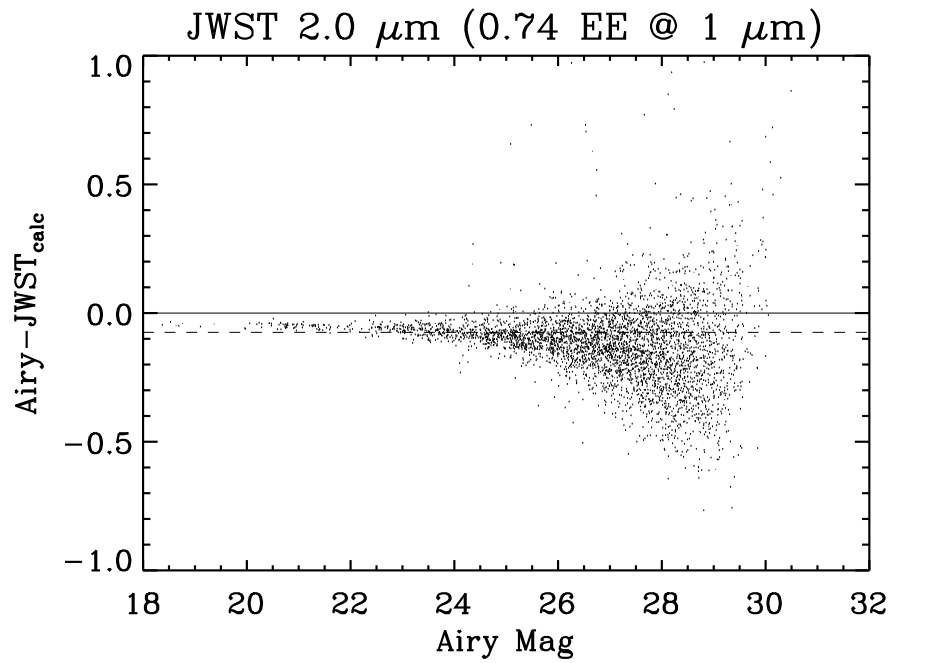

Airy–JWST: EE(1.0μm)=0.74

Δm_{Tot}

0.7 μm

1.0 μm

2.0 μm

m_{Tot} bias still significant, and remains –5% at very bright fluxes, and for EE=0.74 is slightly worse

at 0.7 μm & 1.0 μm than at 2.0 μm, because of by larger PSF-wings. Better λ/D thus loses out to the poorer PSF-wings and undersampling.

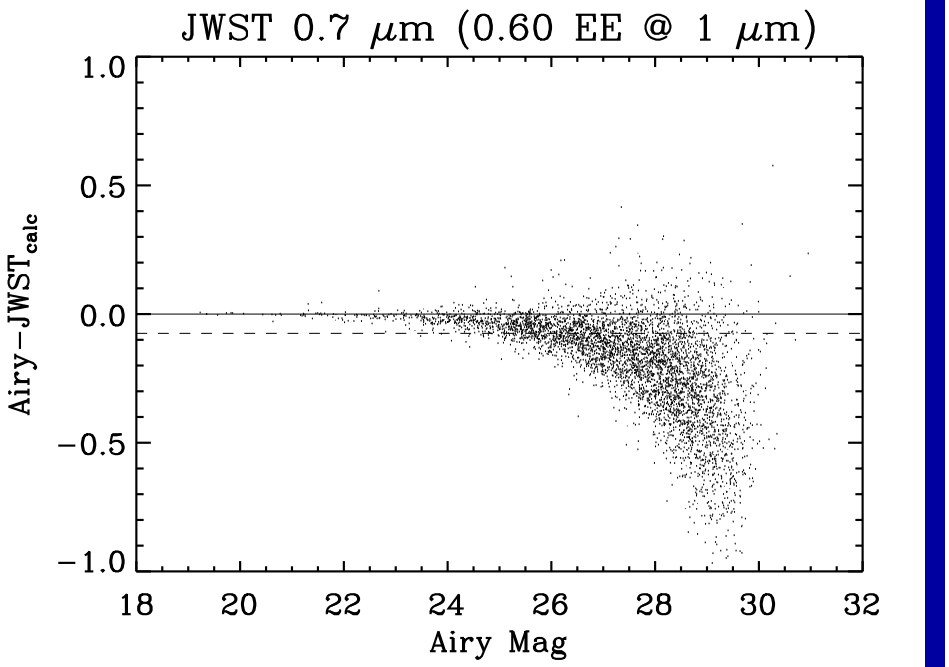

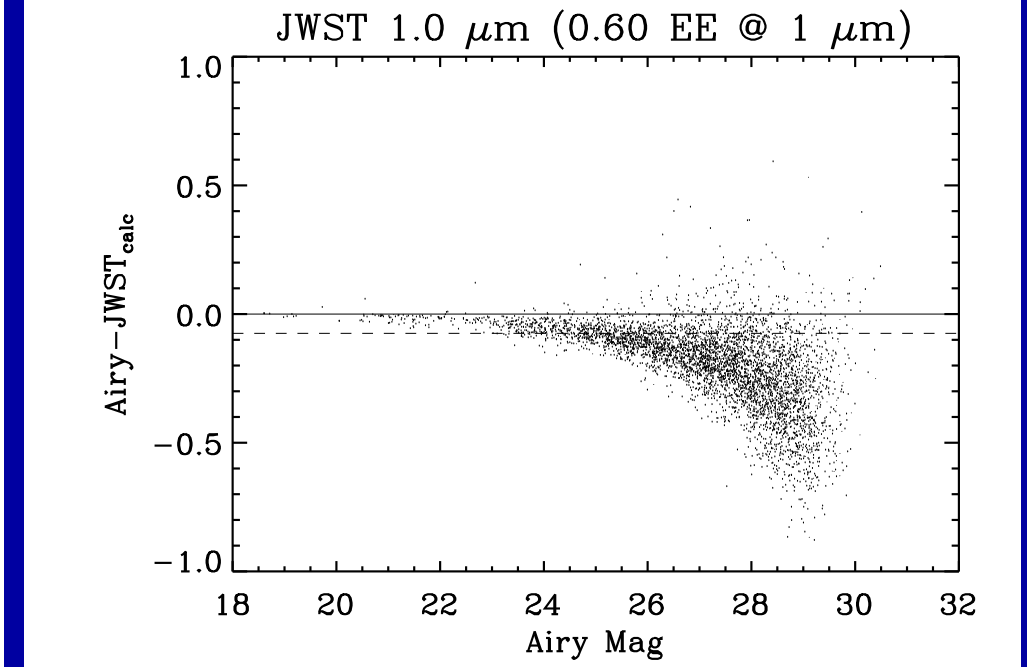

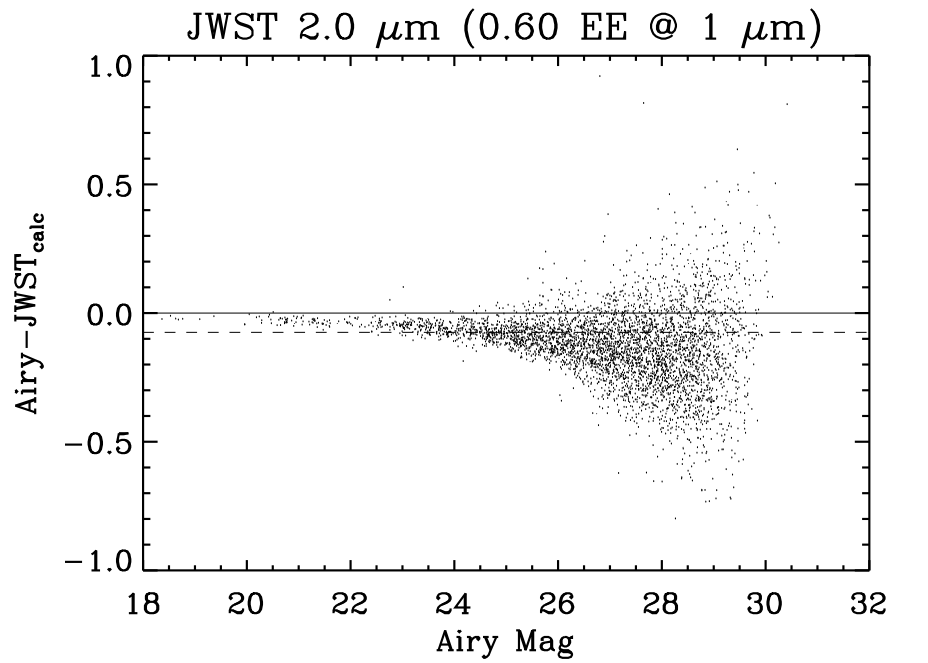

Airy–JWST: EE(1.0μm)=0.60

Δm_{Tot}

0.7 μm 1.0 μm

2.0 μm

For EE=0.60, the m_{Tot} bias gets more significant, especially at 0.7 and 1.0 μm. Any gains from better λ/D at 0.7–1.0 μm lose out to poorer PSF wings and undersampling. The 2.0 μm performance is held $\sim$constant (as spec-ed).

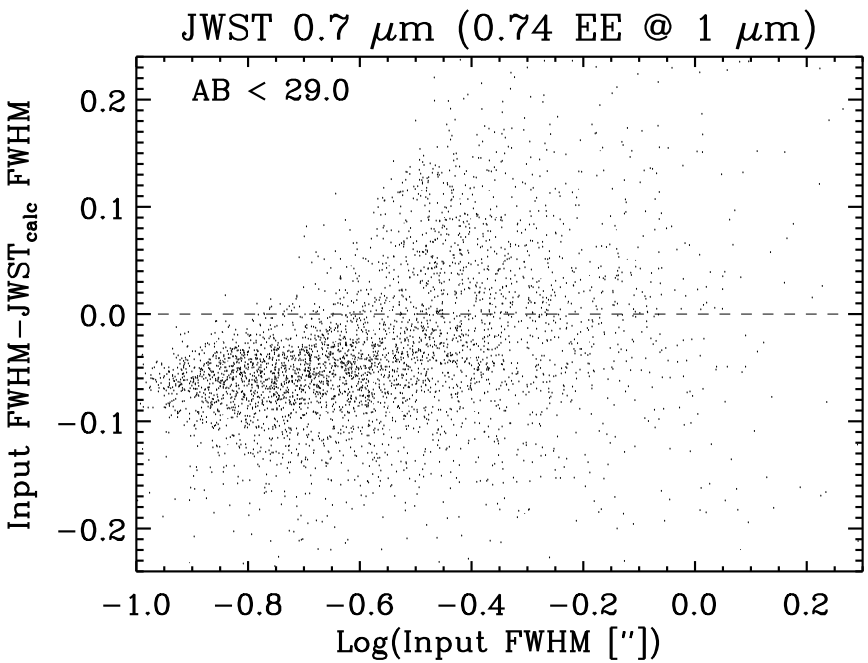

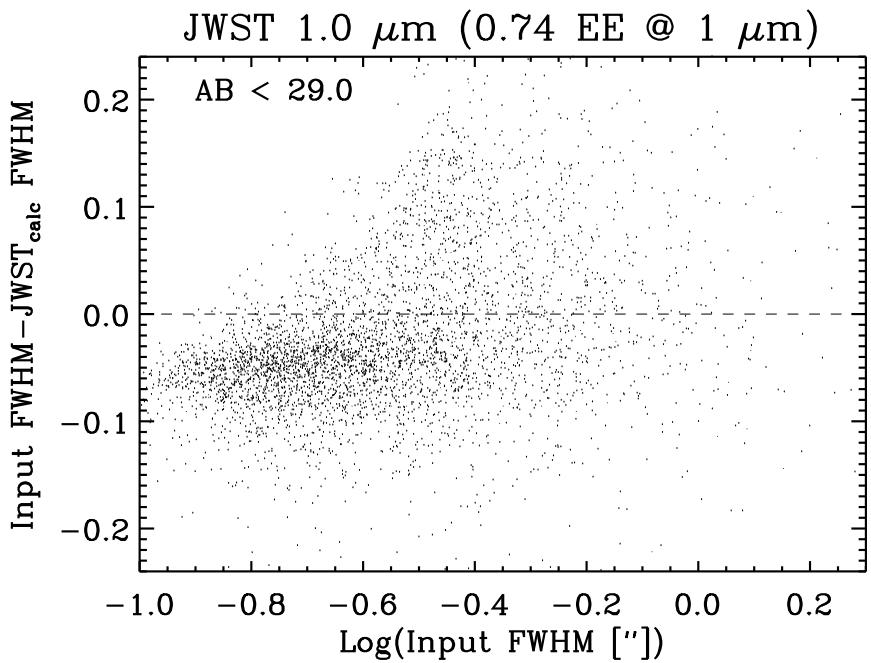

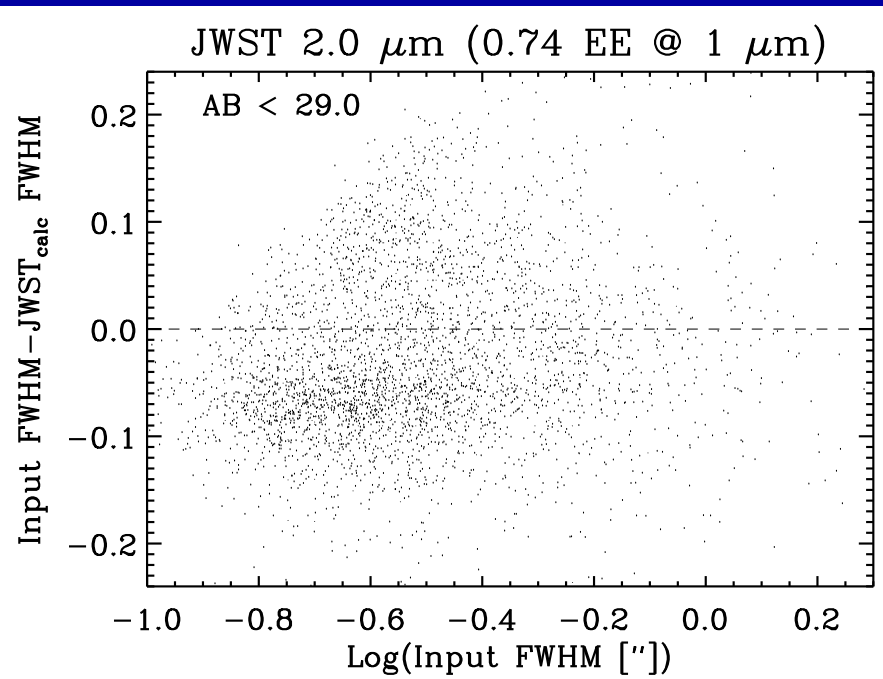

Input–JWST: EE(1.0μm)=0.74

ΔFWHM

0.7 μm 1.0 μm

2.0 μm

The FWHM bias is significant, and is –0$''$.06 on average, but it is slightly smaller & tighter at 1.0 & 0.7 μm,

due to the better JWST λ/D, *and* the smaller input ACS-sizes (ACS λ/D). The latter bias must be addressed by simulating artificial objects.

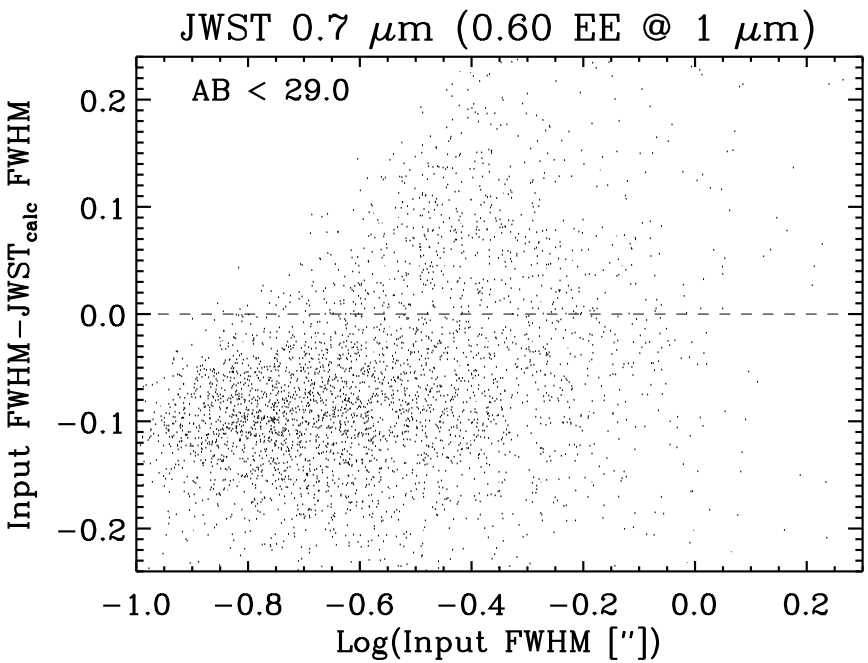

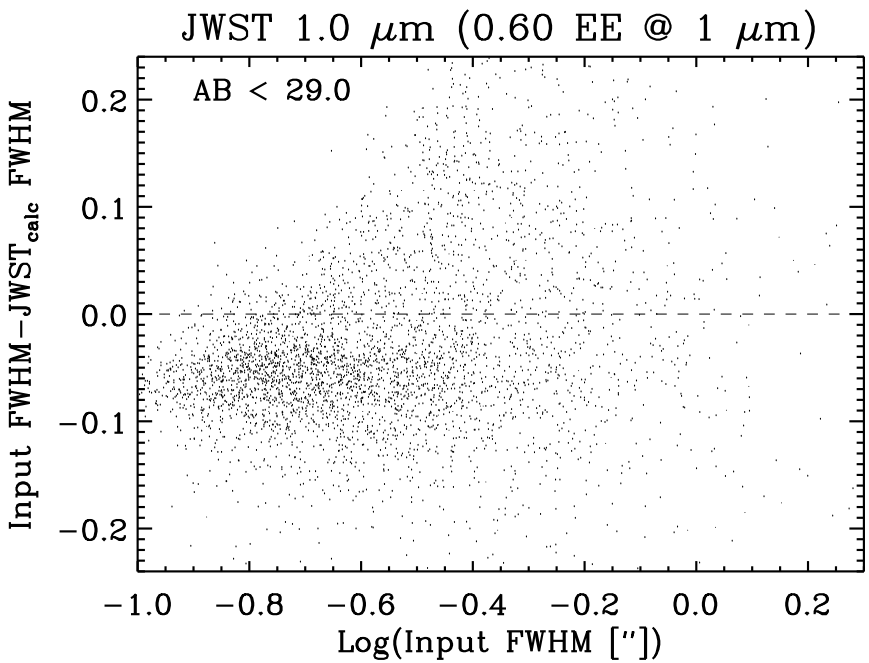

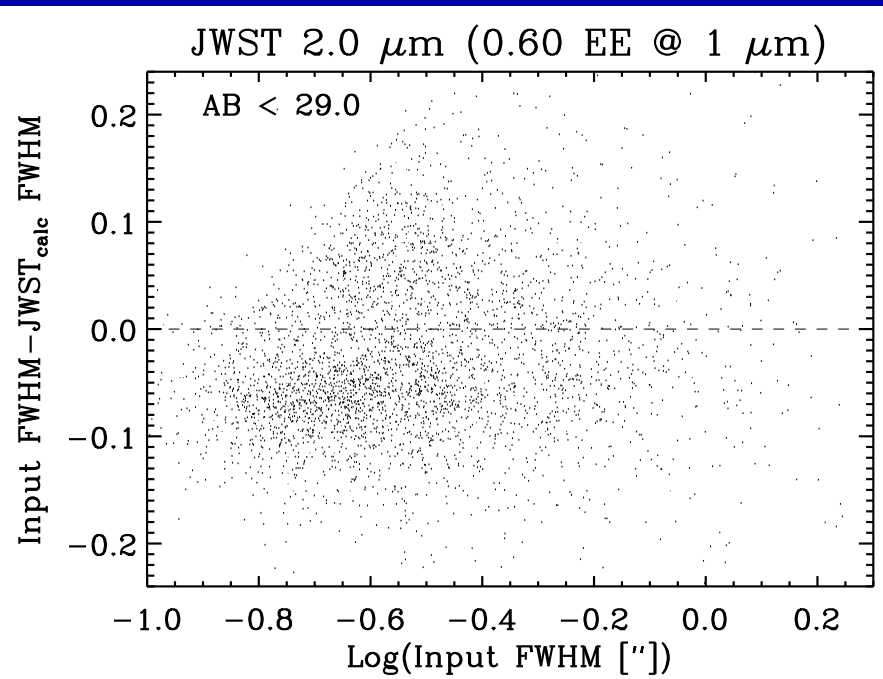

Input–JWST: EE(1.0μm)=0.60

ΔFWHM

0.7 μm

1.0 μm

2.0 μm

For EE=0.60, the FWHM bias gets worse with a wider error-distribution, especially at 0.7 & 1.0 μm.

The ability to measure sizes and the corresponding point source sensitivity thus quickly get worse at shorter λ when going from EE=0.74 to 0.60.

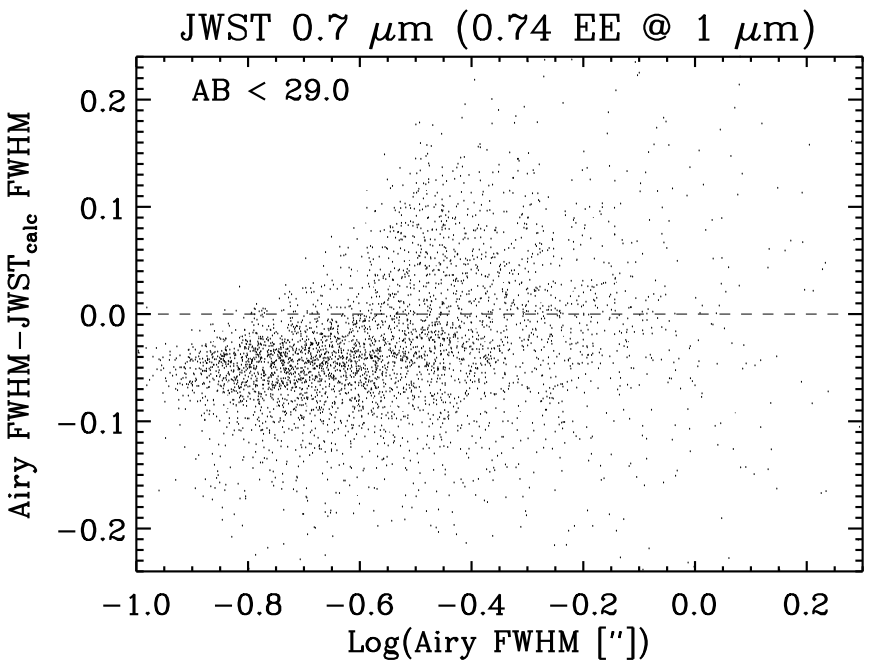

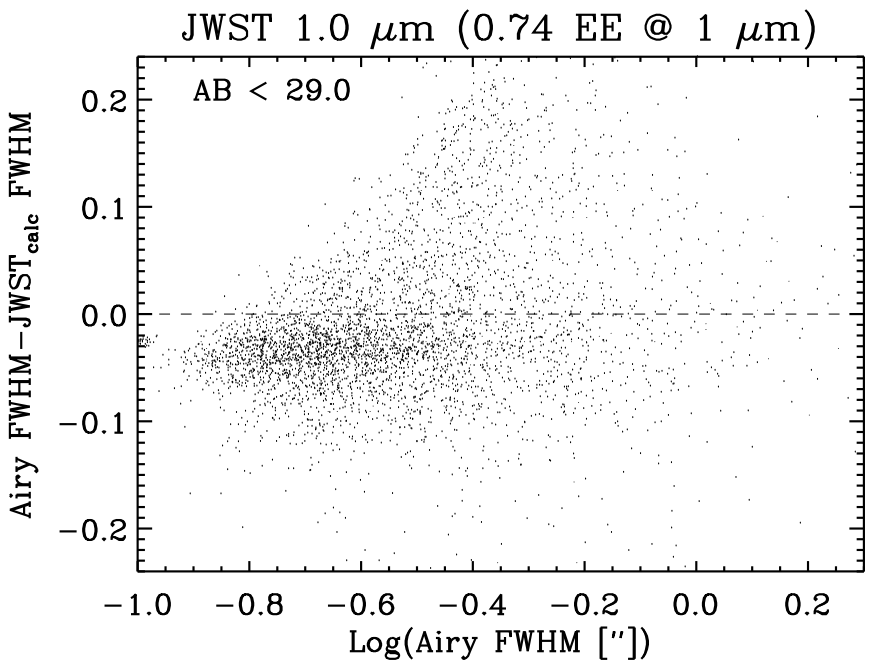

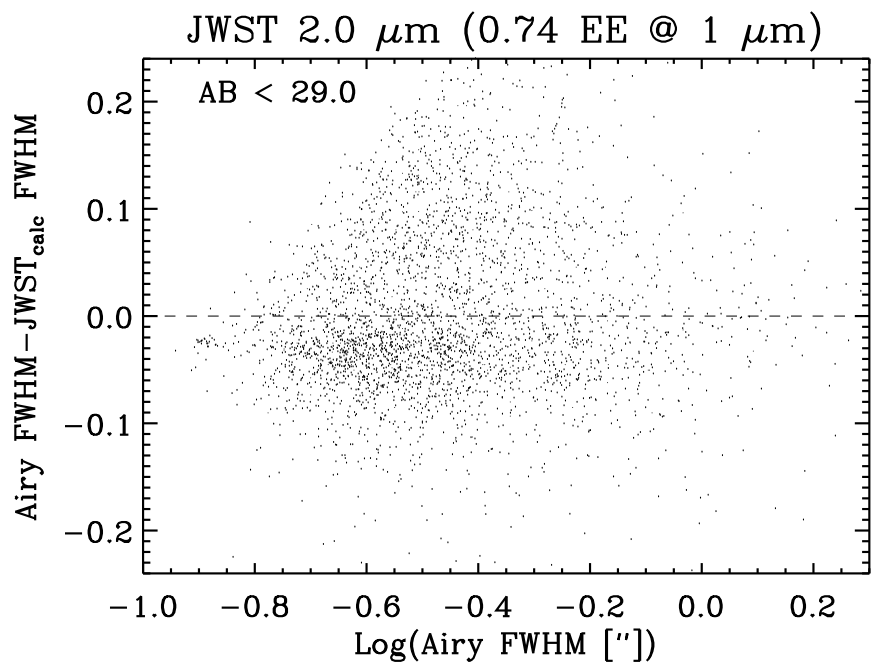

Airy–JWST: EE(1.0μm)=0.74

ΔFWHM

0.7 μm 1.0 μm

2.0 μm

The FWHM bias is significant, and is –0$''$.06 on average, but it is slightly smaller & tighter at 1.0 & 0.7 μm,

due to the better JWST λ/D, *and* the smaller input ACS-sizes (ACS λ/D). The latter bias must be addressed by simulating artificial objects.

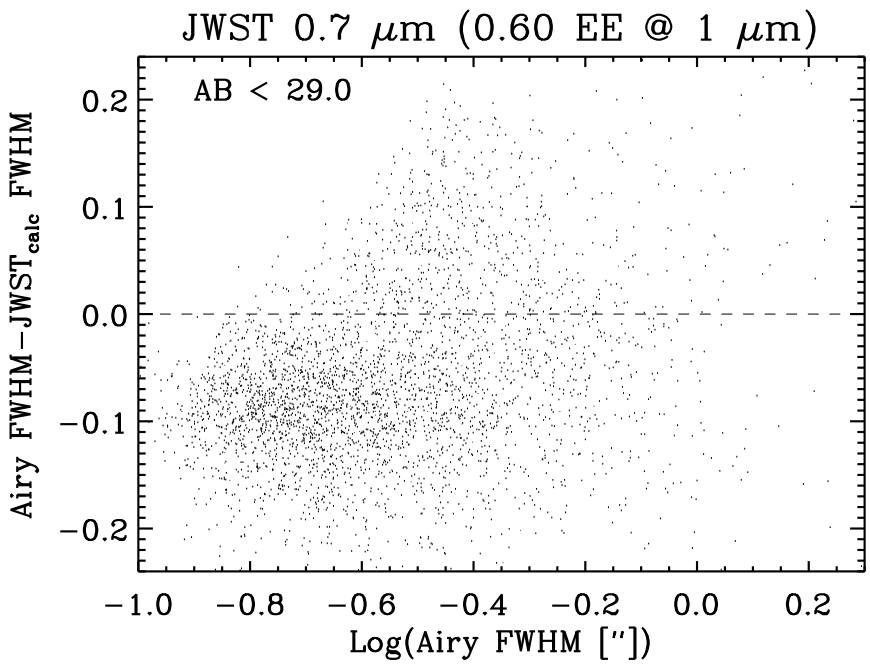

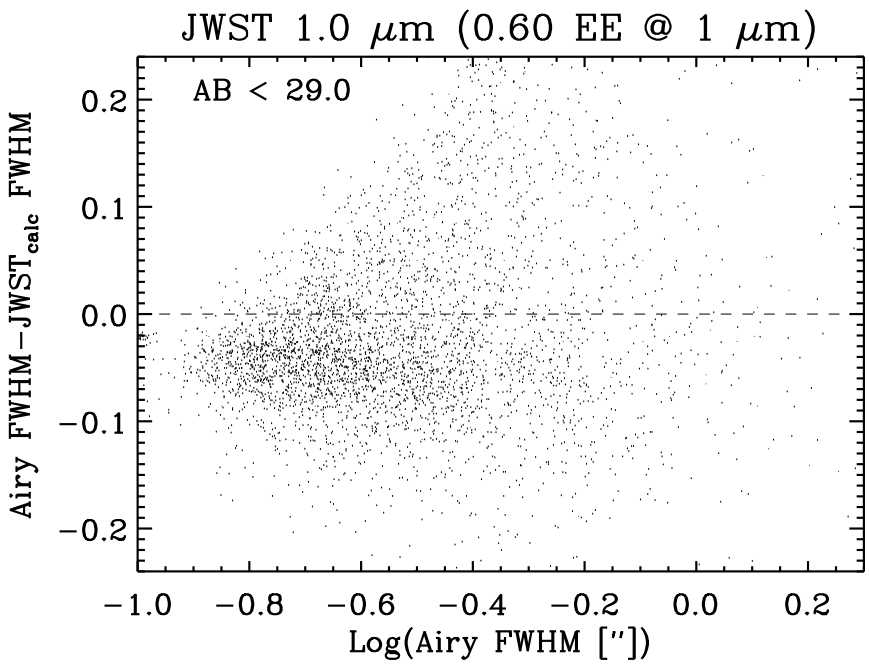

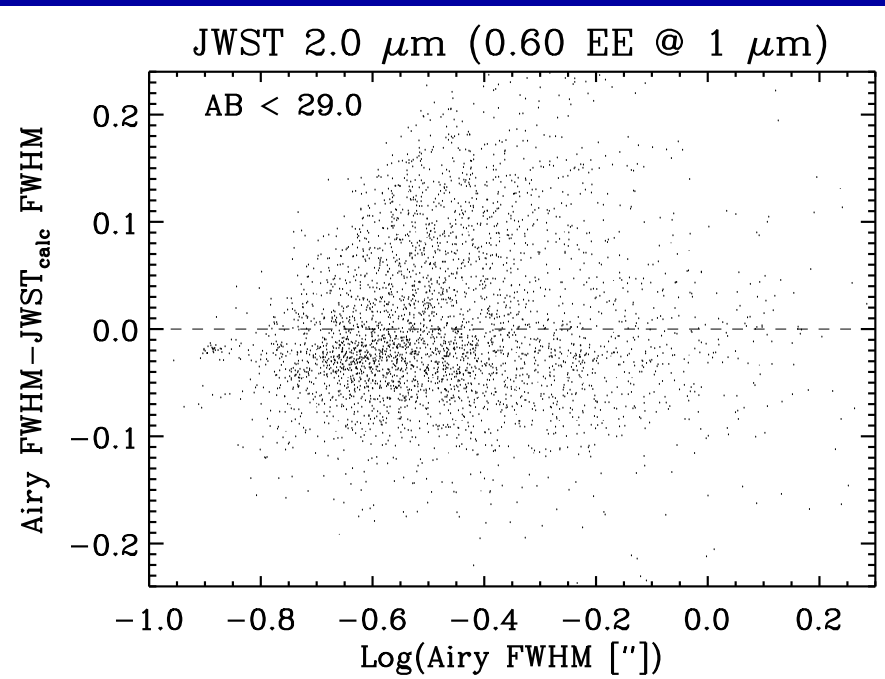

Airy–JWST: EE(1.0μm)=0.60

ΔFWHM

0.7 μm

1.0 μm

2.0 μm

For EE=0.60, the FWHM bias gets worse with a wider error-distribution, especially at 0.7 & 1.0 μm.

The ability to measure sizes and the corresponding point source sensitivity thus quickly get worse at shorter λ when going from EE=0.74 to 0.60.

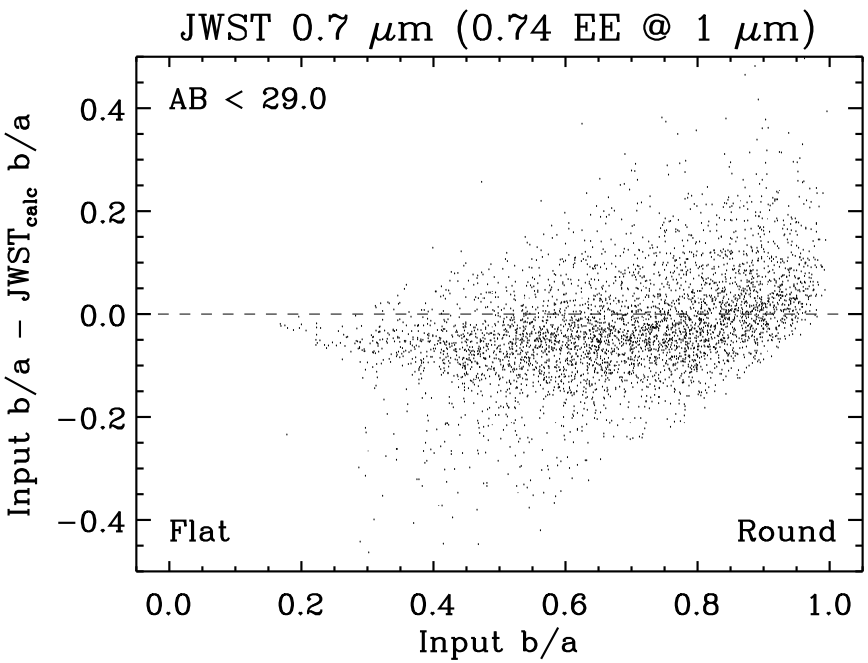

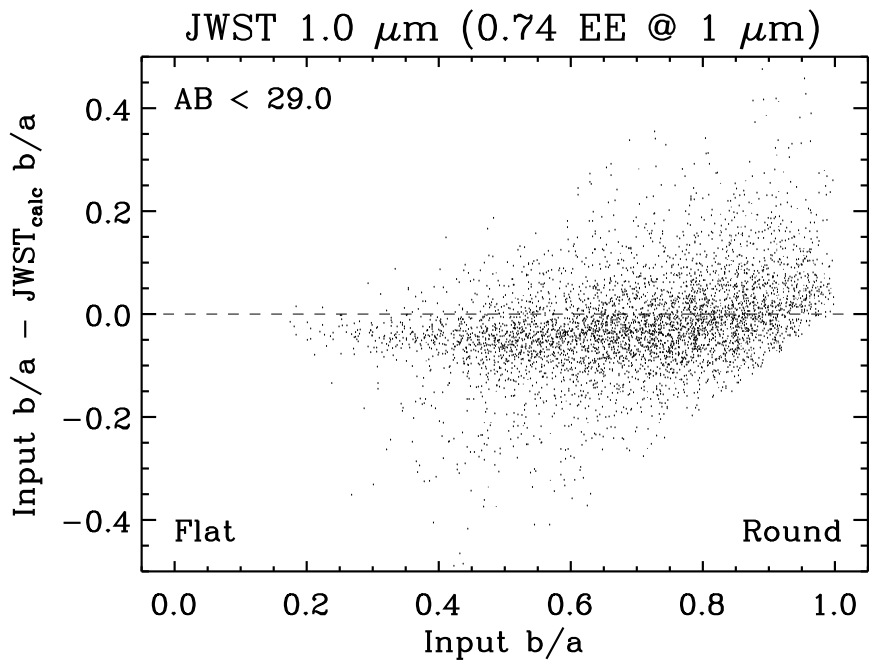

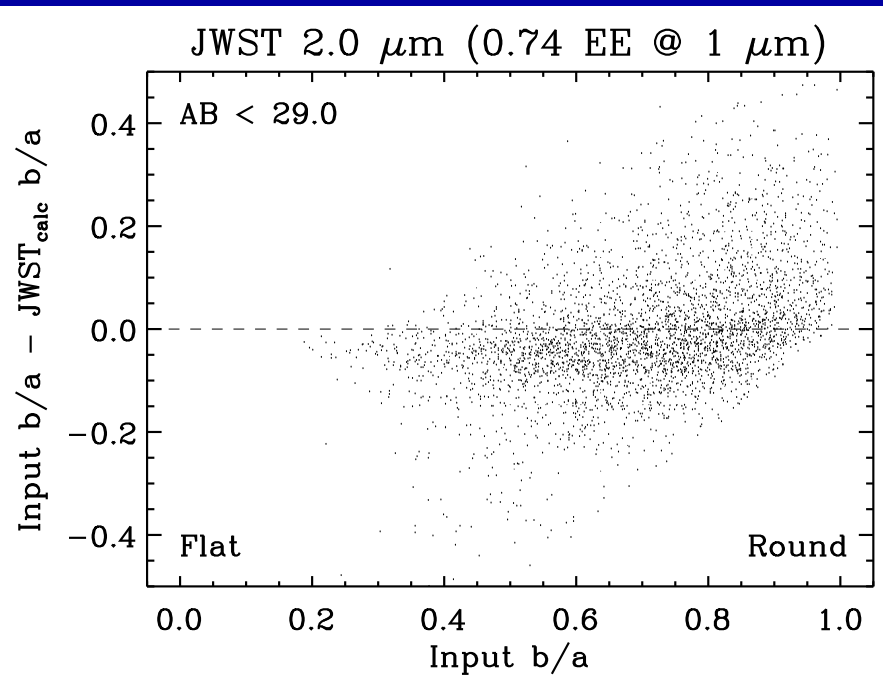

Input–JWST: EE(1.0μm)=0.74

Δb/a

0.7 μm 1.0 μm

2.0 μm

The b/a bias is as usual:

Truly flat objects get a bit rounder,

& truly round objects a bit flatter.

For EE=0.74, this bias is perhaps a bit tighter at 1.0 μm, due to the better λ/D, but at 0.7 μm the PSF-wings become the dominant factor.

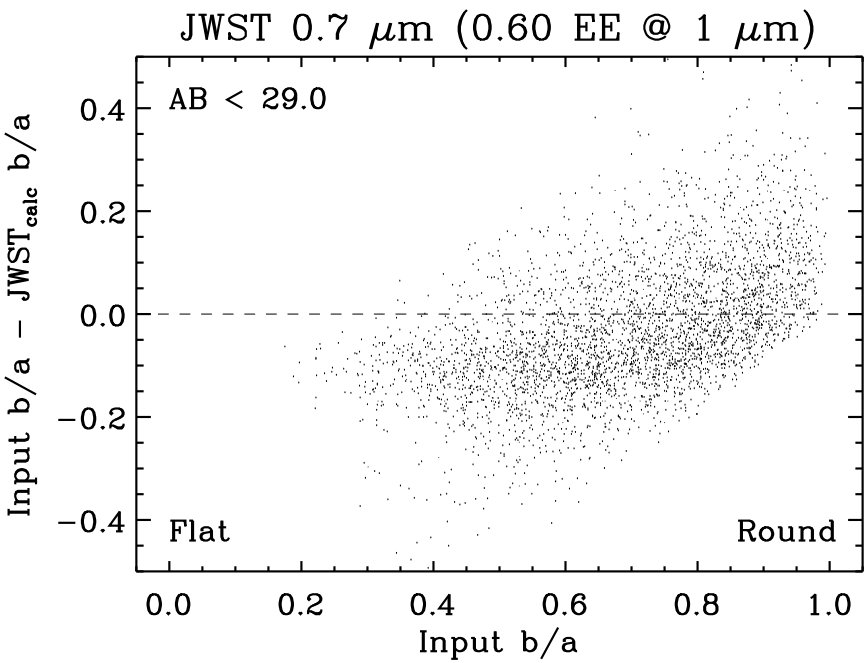

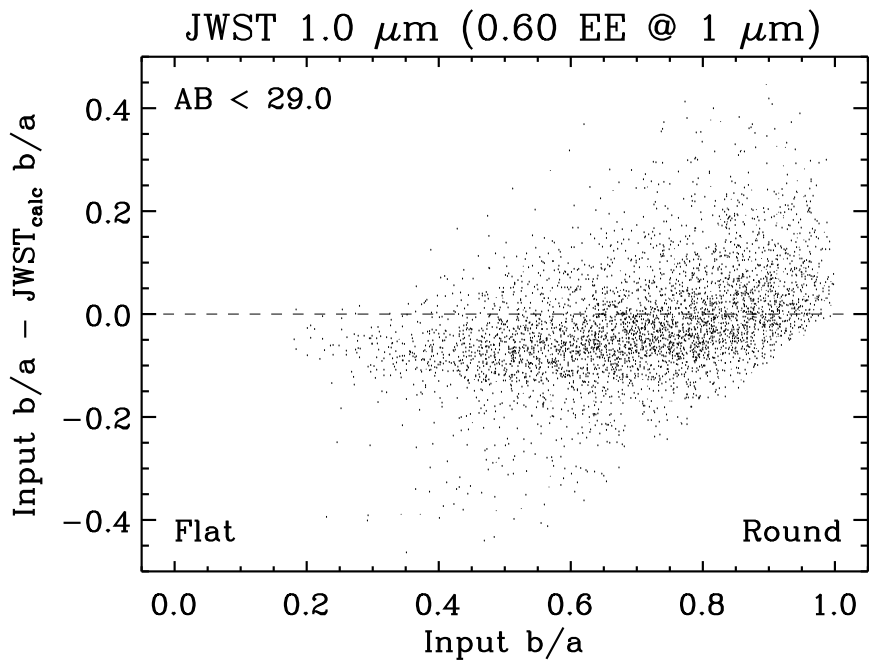

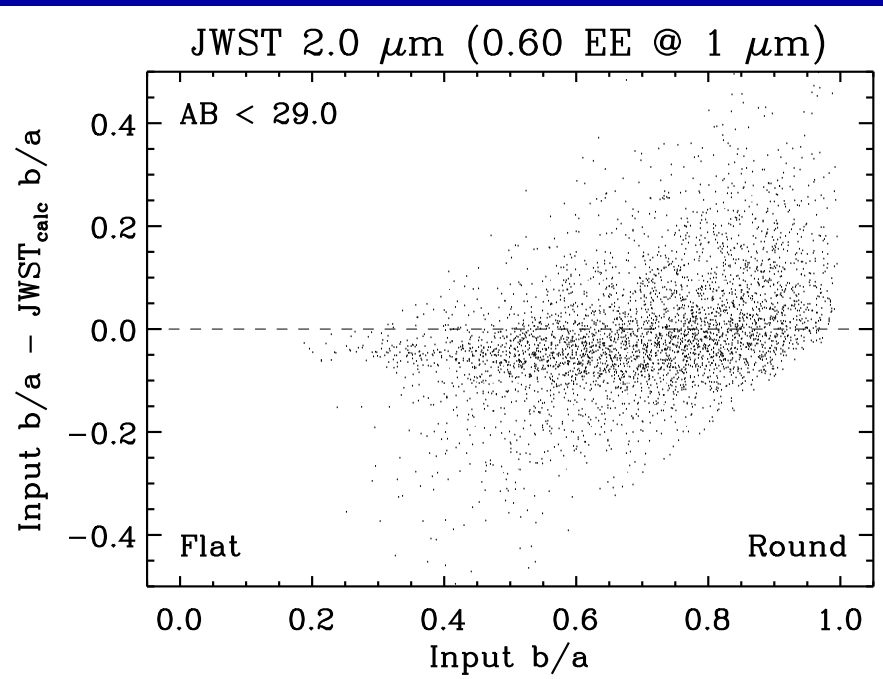

Input–JWST: EE(1.0μm)=0.60

Δb/a

0.7 μm 1.0 μm

2.0 μm

For EE=0.60, same 2.0 μm b/a bias:

Truly flat objects get a bit rounder,

& truly round objects a bit flatter.

But for EE=0.60, this bias gets worse at 1.0 μm and especially at 0.7 μm, so the better λ/D quickly loses out to the larger PSF-wings.

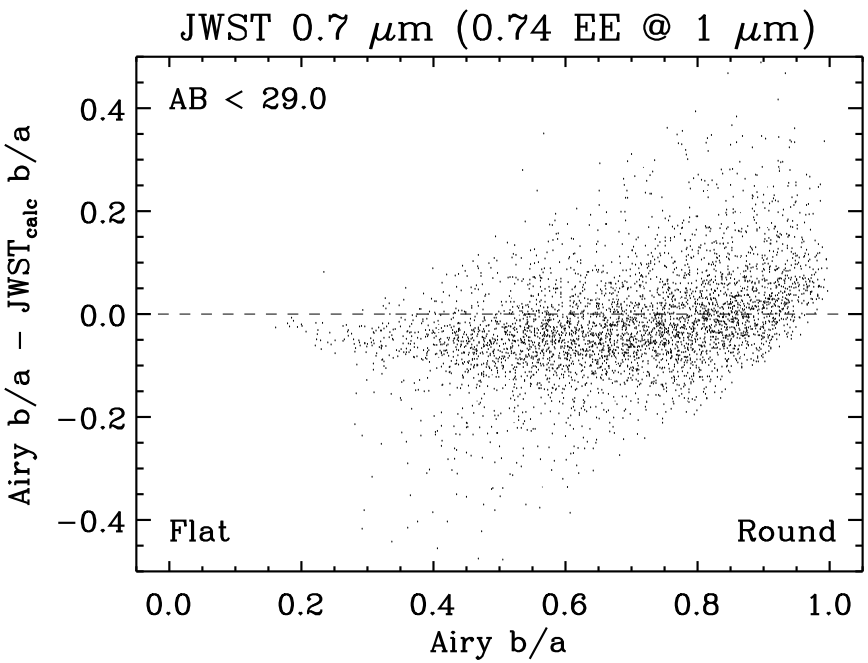

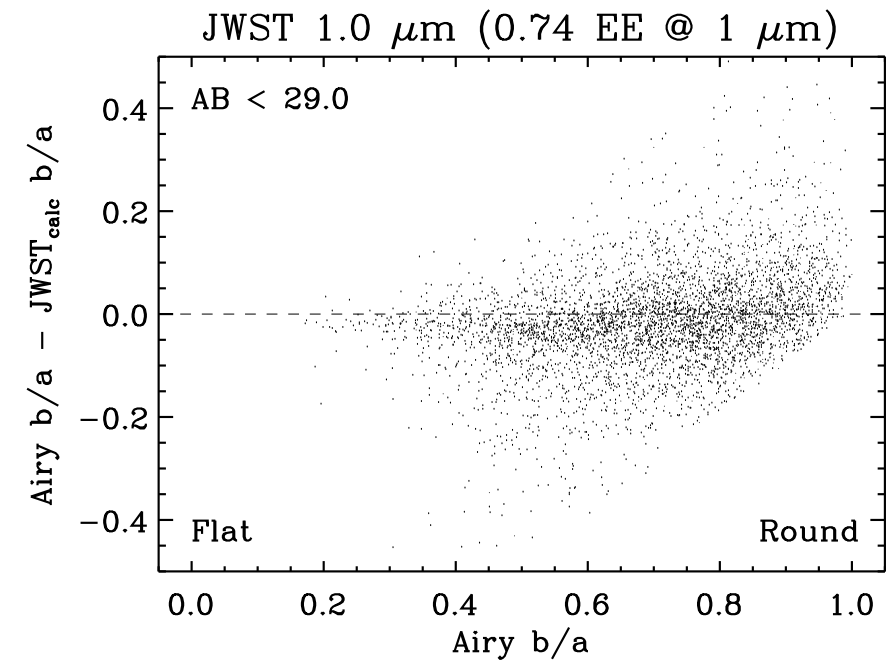

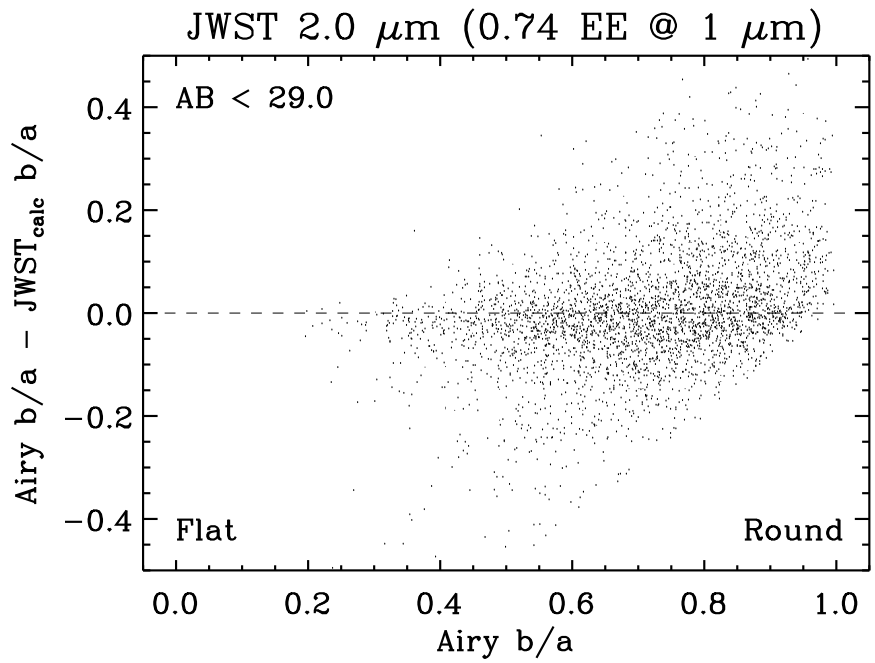

Airy–JWST: EE(1.0μm)=0.74

Δb/a

0.7 μm 1.0 μm

2.0 μm

The b/a bias remain as usual:

Truly flat objects get a bit rounder,

& truly round objects a bit flatter.

For EE=0.74, this bias is perhaps a bit tighter at 1.0 μm, due to the better λ/D, but at 0.7 μm the PSF-wings become the dominant factor.

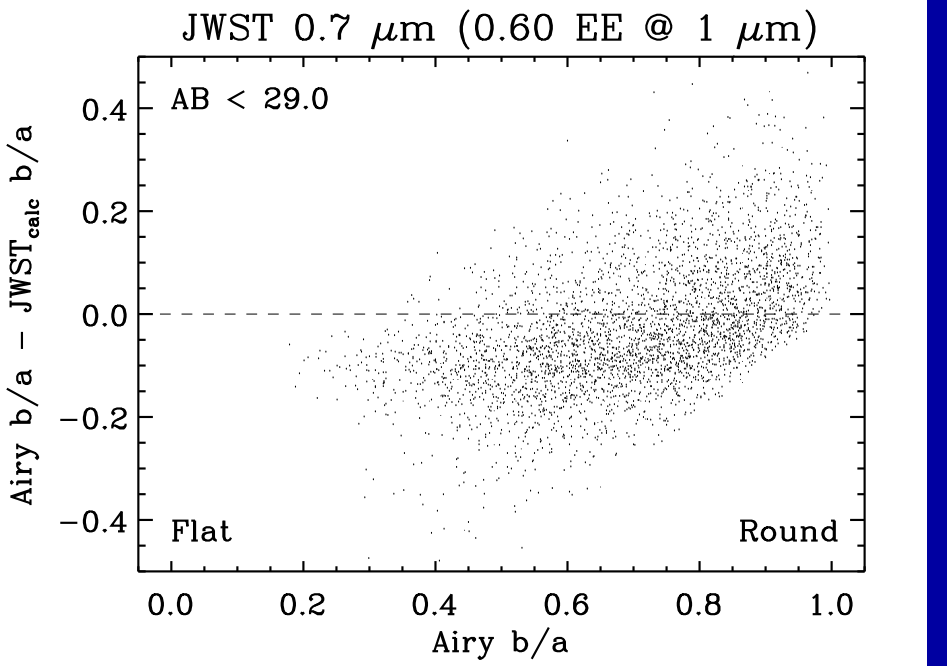

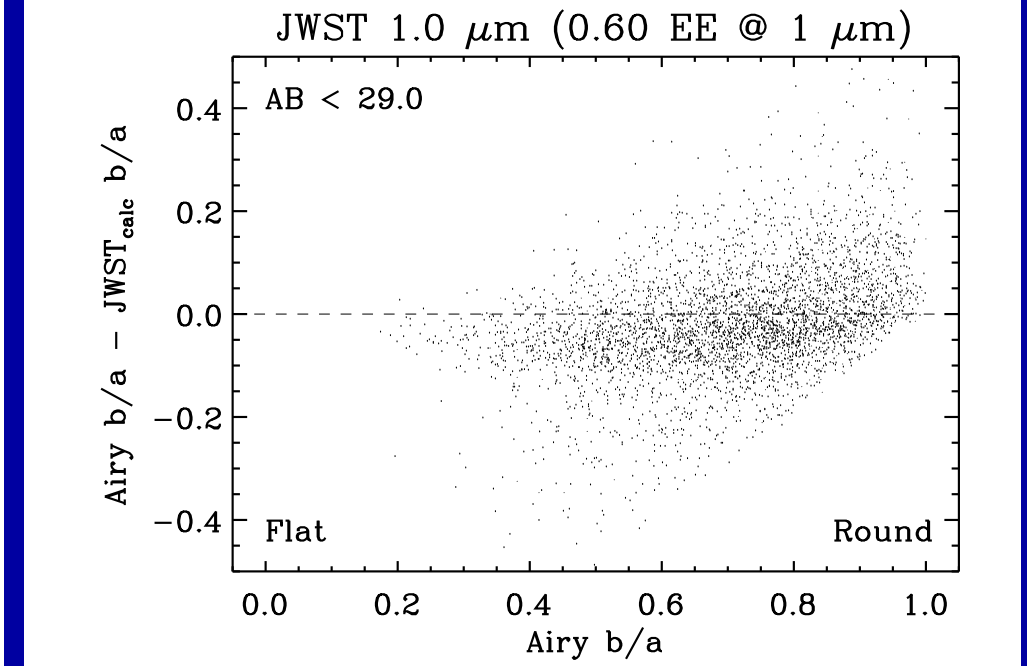

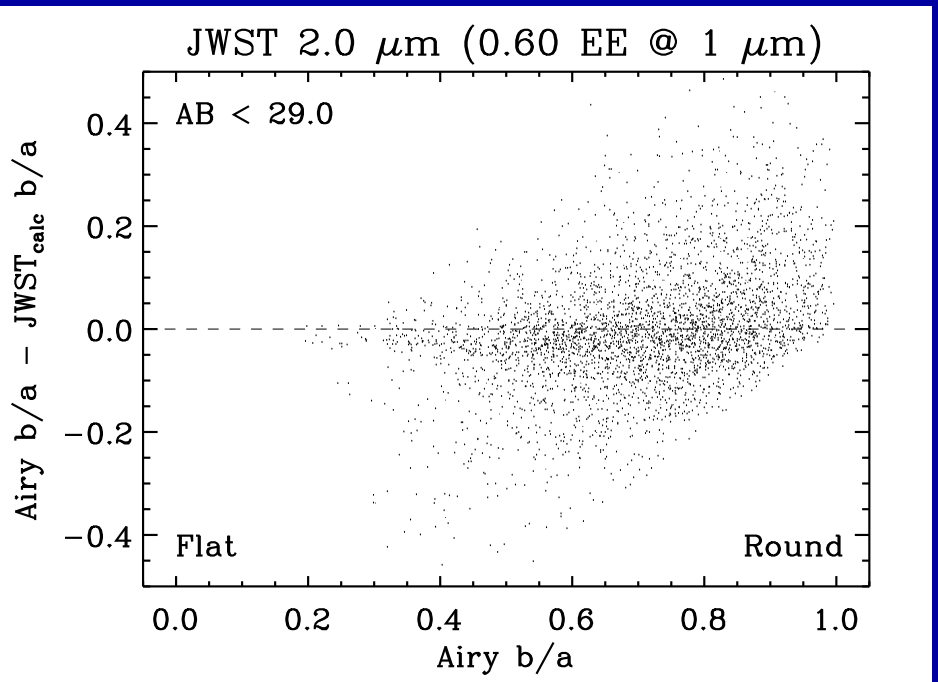

Airy–JWST: EE(1.0μm)=0.60

Δb/a

0.7 μm

1.0 μm

2.0 μm

For EE=0.60, same 2.0 μm b/a bias:

Truly flat objects get a bit rounder,

& truly round objects a bit flatter.

But for EE=0.60, this bias gets worse at 1.0 μm and especially at 0.7 μm, so the better λ/D quickly loses out to the larger PSF-wings.

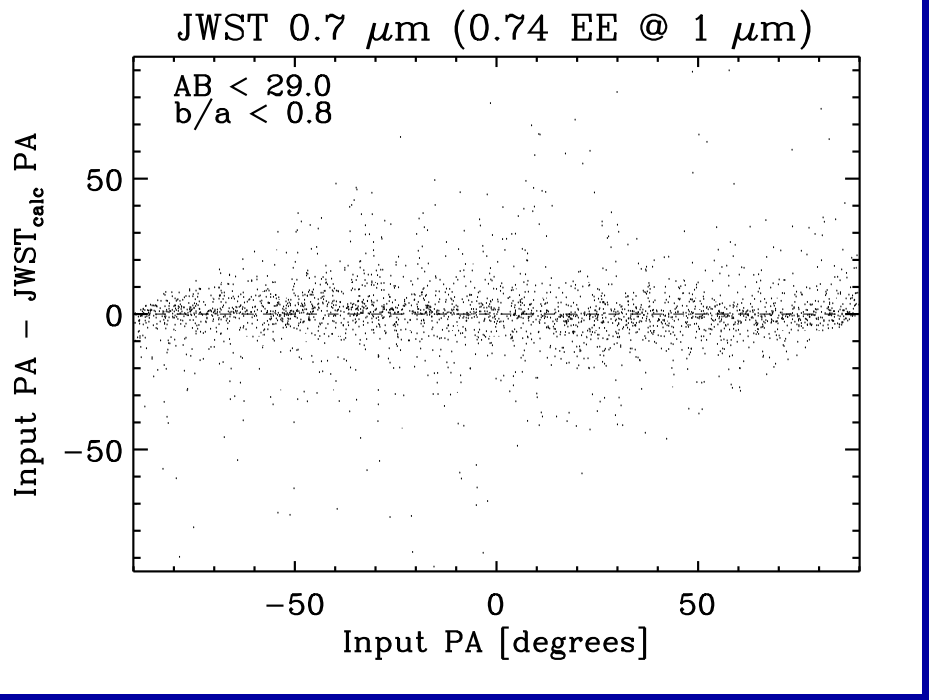

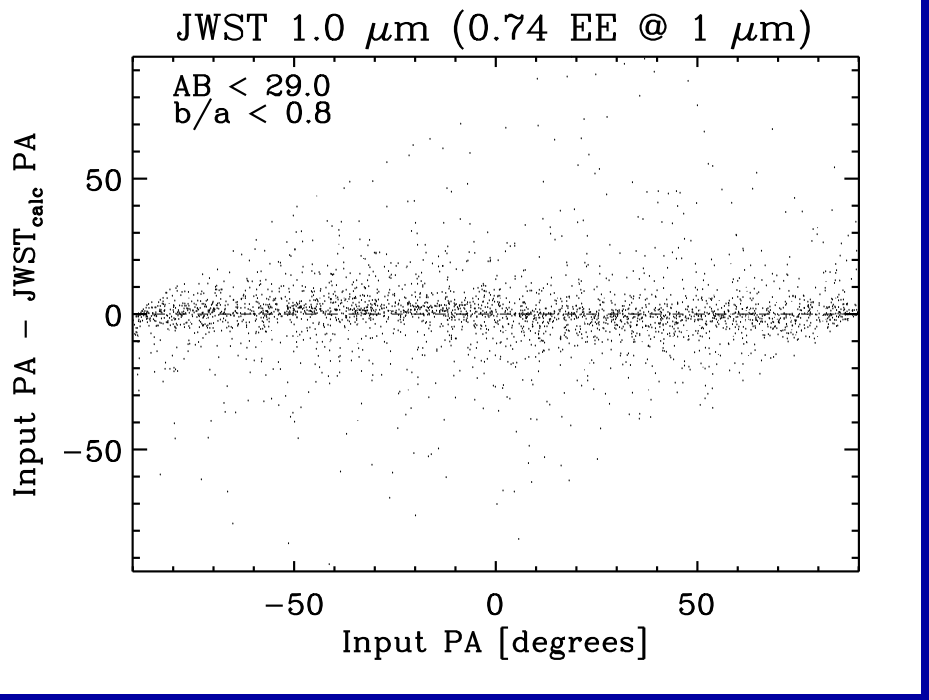

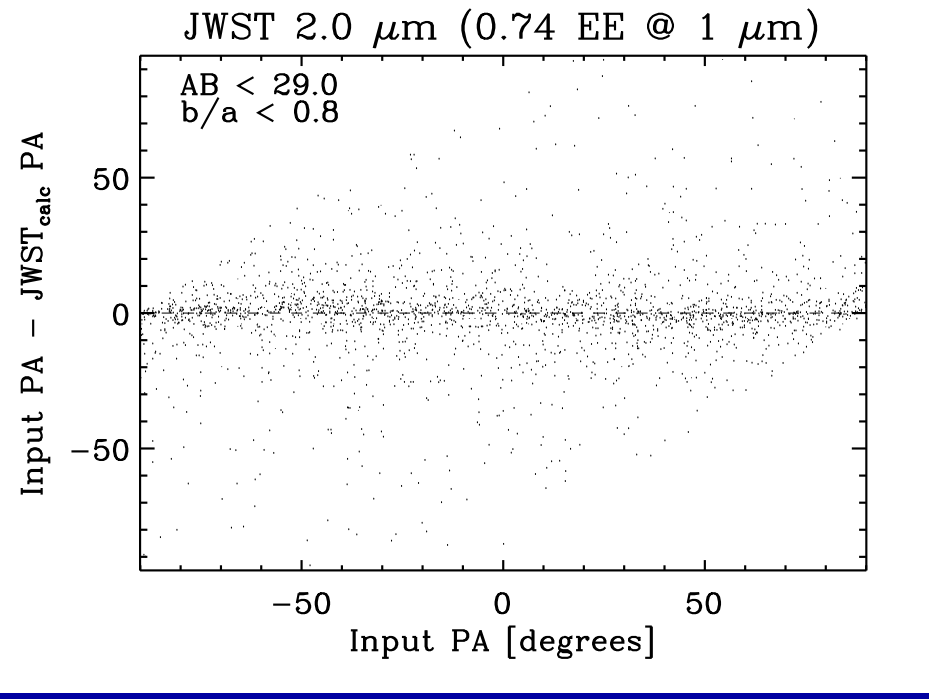

Input–JWST: EE(1.0μm)=0.74

ΔPA

0.7 μm

1.0 μm

2.0 μm

The PA-bias is small & random, and at 0.7 & 1.0 μm not much worse. This is because the outer isophotes are used for PA-determination, independently at all three wavelengths, which does not deteriorate until gross power is put in the PSF-wings.

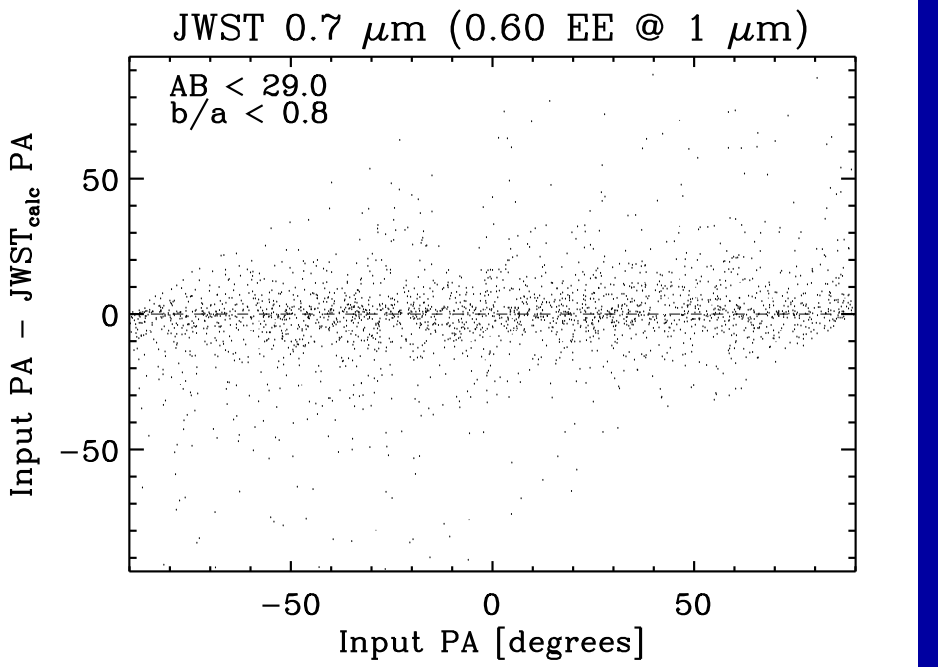

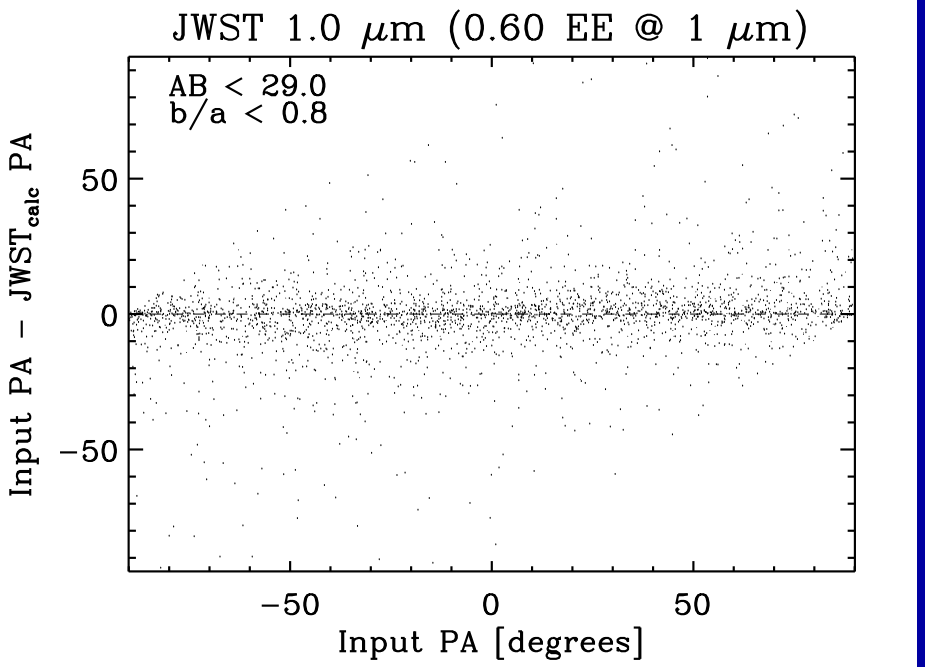

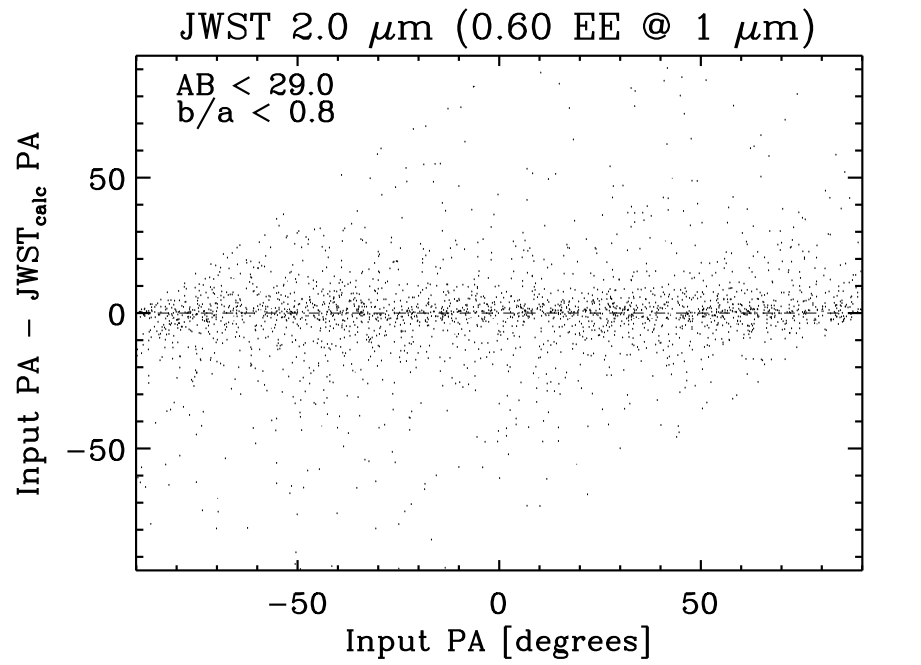

Input–JWST: EE(1.0μm)=0.60

ΔPA

0.7 μm

1.0 μm

2.0 μm

For EE=0.60 PA-bias remains small, but at 0.7 & 1.0 μm the random PA-errors get somewhat larger.

At EE=0.60, these larger random PA errors smooth-out the slight PA-wiggles seen at short λ's for EE=0.74, which are caused by PSF-wiggles.

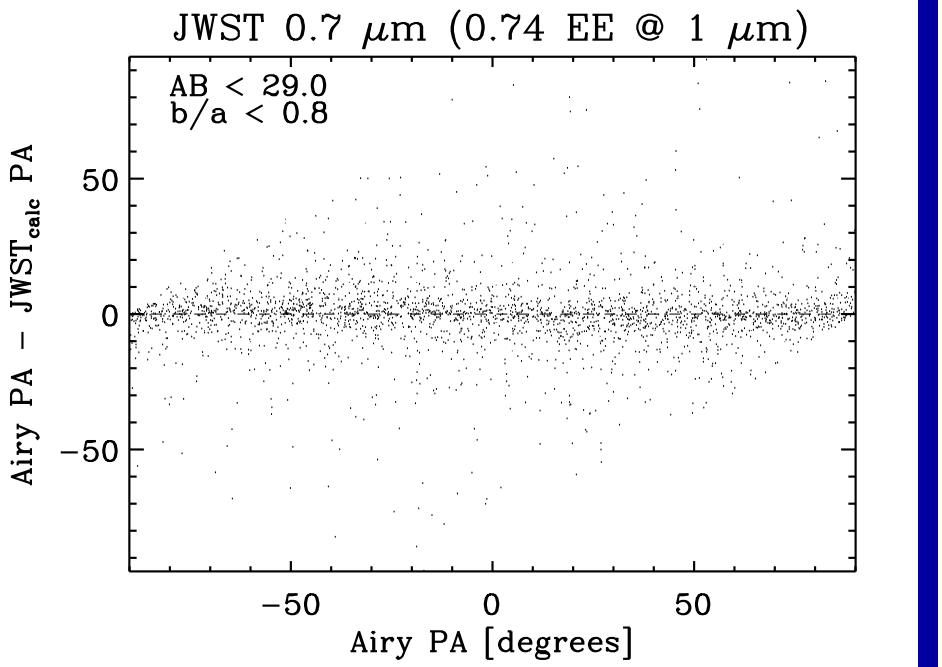

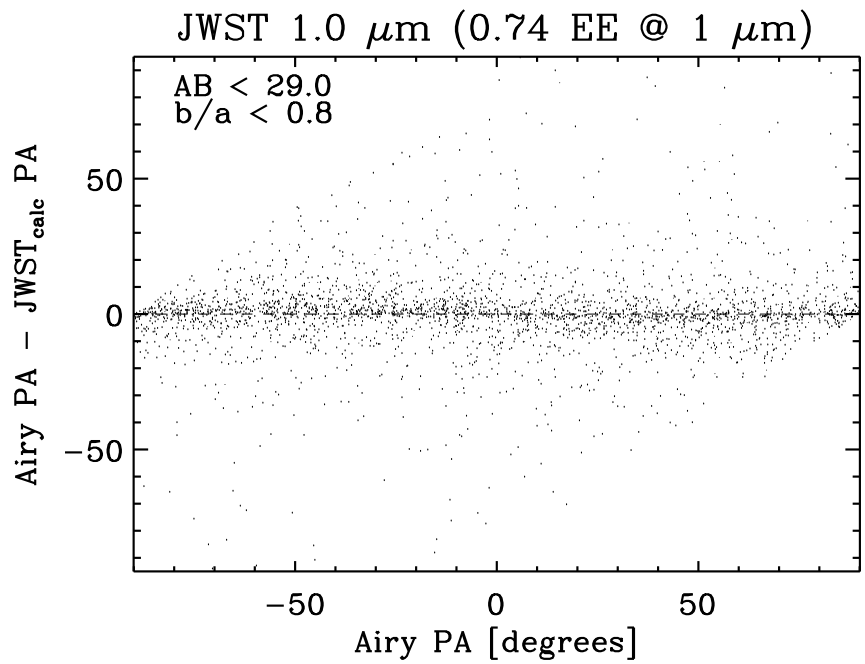

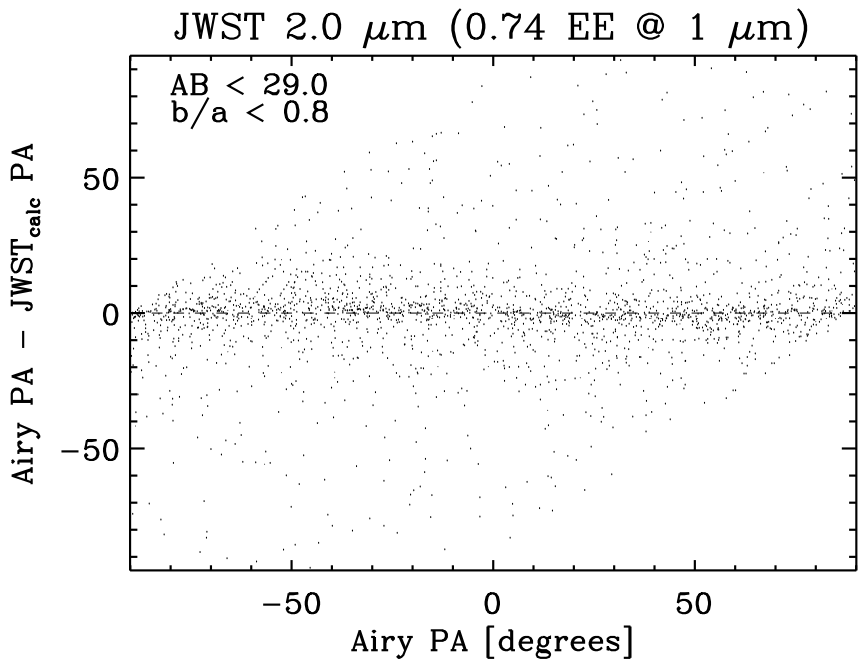

Airy–JWST: EE(1.0μm)=0.74

ΔPA

0.7 μm

1.0 μm

2.0 μm

The PA-bias remains small & random, & at 0.7 & 1.0 μm not much worse. This is because the outer isophotes are used for PA-determination, independently at all three wavelengths, which does not deteriorate until gross power is put in the PSF-wings.

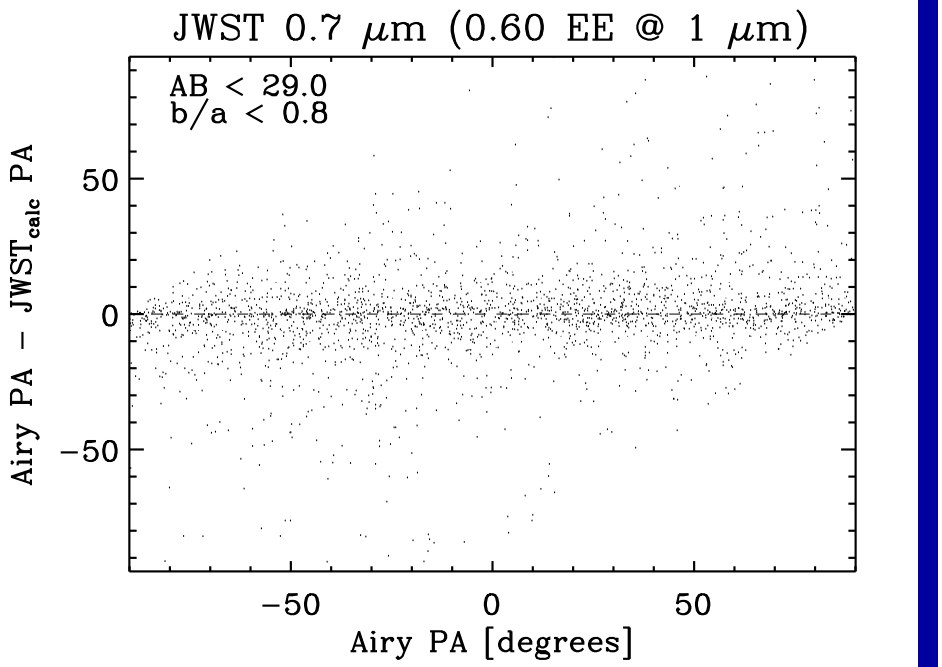

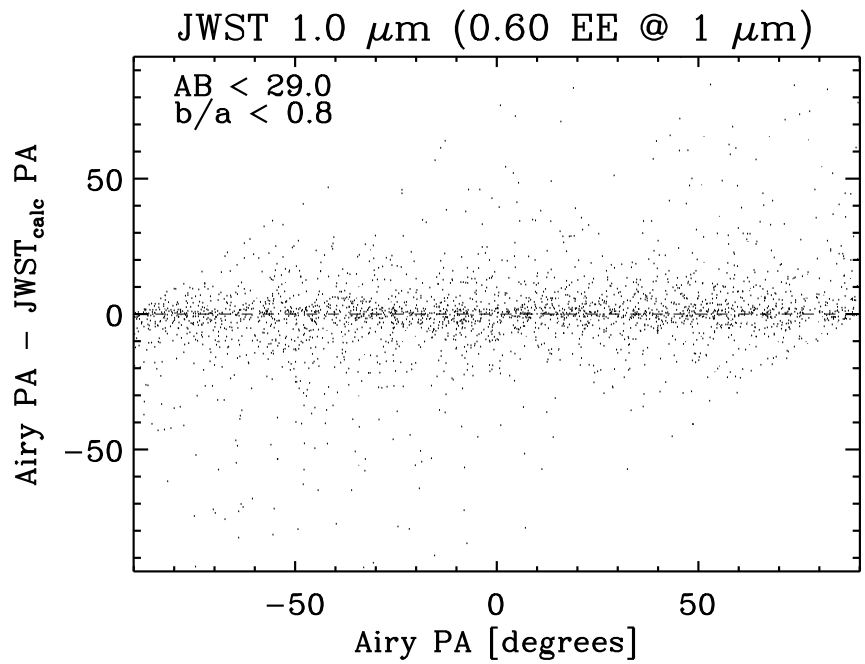

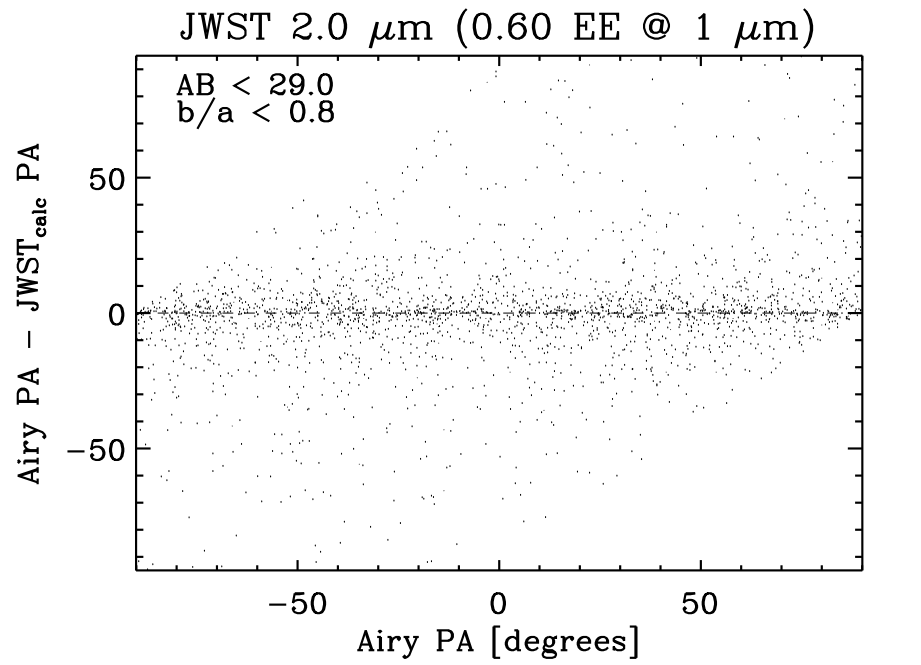

Airy–JWST: EE(1.0μm)=0.60

ΔPA

0.7 μm

1.0 μm

2.0 μm

For EE=0.60 PA-bias remains small, but at 0.7 & 1.0 μm the random PA-errors get somewhat larger.

At EE=0.60, these larger random PA errors smooth-out the slight PA-wiggles seen at short λ's for EE=0.74, which are caused by PSF-wiggles.

(6) Conclusions

JWST PSF simulations on the real HUDF data shows that faint galaxy parameters are affected as following:

• (1) PA-bias is modest and largely random, with random errors increasing for decreasing EE. Systematics are small at 0.7, 1.0, and 2.0 μm because the outer isophotes are used for PA-determination, which does not deteriorate until significant power is put into the PSF-wings.

• (2) The m_{Tot}, FWHM, and b/a-biases are more significant and caused by algorithm's response to JWST's PSF-wings. For real JWST images, this bias is non-zero even for good EE-values ($\gtrsim$0.7), and has to be modeled and removed.

• (3) Going from EE=0.74 to EE=0.60, the m_{Tot}, FWHM, and b/a-biases become more significant — and their error distributions get wider — at 0.7 and 1.0 μm, but are held roughly constant at 2.0 μm (as spec-ed).

(6) Conclusions (continued)

• (4) At the brightest fluxes (AB$\lesssim$22), the m_{Tot} bias is still $\simeq$–5% or –0.05 mag. This is a remaining (small) aperture correction, that also exists for HST/WFPC2 and ACS, and should be incorporated in the JWST zero-points as a routine correction in the data pipeline.

• (5) For EE=0.74, the 1.0 μm performance for m_{Tot} and FWHM (and perhaps also for b/a) is slightly better than at 2.0 μm due to the better λ/D, but for EE=0.60 this is no longer the case. From EE=0.74 to EE$\Rightarrow$0.60, any λ/D advantages quickly lose out to the larger PSF-wings and undersampling.

• There is thus perhaps some MODEST room to explore in EE-parameter space to save mission cost without killing many of JWST's science goals.

• CRITICAL CAVEAT 1: Must confirm this by either successfully deconvolving out ACS-PSF, or by simulating artificial sources.

• CRITICAL CAVEAT 2: Must consult with NIRSpec team to make sure that this does not unduly affect the (MEMS) spectroscopic performance.